Metal Ion Promoted Hydration of Pendant Alkenes and Its Possible Relationship to Aconitase

Lawrence R. Gahan, Jack M. Harrowfield, Anthony J. Herlt, Leonard F. Lindoy, Peter O. Whimp, and Alan M. Sargeson*

Contribution from the Research School of Chemistry, Australian National University, Canberra A.C.T. 2600, Australia. *Received October 19, 1984*

Abstract: The hydration of coordinated carboxyalkenes has been studied by using bis(1,2-ethanediamine)cobalt(III) complexes with either methyl maleate or ethyl fumarate coordinated cis to an aqua molecule. Upon removal of a proton from the aqua ligand (pK_a 7.14) under pH-stat conditions, the $[Co(en)_2(OH)(methylmaleato)]^+$ ion undergoes a rapid intramolecular cyclization reaction ($k = 3.4 \times 10^{-2}$ s^{-1} at pH 8.05, 25 °C, μ = 1.0 M $NaClO_4$) to produce *cis*-$[Co(en)_2(OH)(methylfumarato)]^+$ and two diastereoisomers of the $[Co(en)_2(methylmalato)]^+$ ion. The intramolecular nature of the cyclization reaction and the exclusive formation of five-membered rings in the chelated malate product have been established by ^{18}O-tracer experiments and a three-dimensional X-ray crystallographic analysis of one of the diastereoisomers (crystal data: $C_9H_{27}Br_2CoN_4O_7$, space group *Cc*, a = 11.200 (4) Å, b = 19.912 (8) Å, c = 11.043 (4) Å, β = 130.66 (2)°, V = 1884.9 Å^3, d_{obsd} = 1.83 (1) g cm^{-3} (d_{calcd} 1.84), Z = 4, N = 128.9, 1628 reflections ($I/\sigma(I) \geq 3.0$), R = 0.054). The reaction is independent of pH between pH 8–10 under pH-stat conditions. In the presence of buffers, the same pattern of reactivity is observed but the rates increase with the acidity of the buffer acid and its concentration (k = 0.11 s^{-1}, pH 8.06, 0.2 M imidazole, 25 °C, μ = 1.0 M $NaClO_4$). A reaction mechanism is discussed in terms of a rate-determining protonation reaction and ring opening of the chelated carbanion generated by the intramolecular attack of a coordinated hydroxo ligand at the olefin (pH 8–10). Above pH 10, a change in the rate-determining step involving attack by a coordinated oxo ligand is suggested. The regio- and stereospecificity and electronic requirements of the cyclization are discussed. Similar chemistry was observed for the analogous *trans*-alkene complex, *cis*-$[Co(en)_2(OH)(ethylfumarato)]^+$ ion, except that the rates were $\sim 10^3$ slower. Much of this chemistry mimics the biochemical observations of the hydration of *cis*-aconitic acid by aconitase, and it implies that binding the aconitic acid and a hydroxide ion to one of the enzyme iron centers would provide a suitable template for the hydration process to give citric and isocitric acids rapidly.

The hydration of alkenes is commonly a sluggish reaction,[1] and stringent conditions are often required, such as high concentrations of either acid or base. By contrast, some enzymes effect rapid hydration of alkenes in near neutral conditions at 25–39 °C. One such enzymic system is aconitase[2] or aconitic acid hydratase, which catalyses the isomerization of citric acid to isocitric acid through the intermediate *cis*-aconitic acid (Figure 1). The enzyme is part of the respiratory cycle, and isocitric acid leads on to 2-ketoglutarate, whereas citric acid is available for fatty acid synthesis and feedback regulation of glycolysis.

Current elegant research[3-7] indicates that the active site of the enzyme contains an $[Fe_4S_4]^{2+}$ cluster. NMR studies[8] have placed the substrates close to a metal ion (within 4 Å), and the presumption is that they are bound to the metal ion. Mössbauer spectroscopy has now shown that the environment of one iron site is drastically altered in the presence of citrate[4] which is consistent with this binding. The dramatic increase of the isomer shift upon substrate binding is interpreted as the ligand environment becoming at least five-coordinate.[4] No amino acid sequence nor structure is available for the enzyme yet,[9] but some detailed studies have been carried out to determine some stereochemical and mechanistic aspects of the enzyme reaction.[10-12]

Of the two CH_2COOH groups in citric acid, only that derived from oxaloacetate is involved in the conversion to *cis*-aconitic acid and isocitric acid, namely the *pro-R*-acetate residue. Moreover, only one proton of the methylene group is involved, and only the 2*R*,3*S* isomer of isocitric acid is a substrate. It has been shown[12] that the proton abstracted from C(2) on citrate is retained by the enzyme and restored to the C(3) atom on isocitrate without exchanging with solvent protons. The oxygen atom involved in the hydration, however, does exchange with solvent oxygen. Trans addition of H^+ and OH^- stereospecifically to *cis*-aconitic acid accommodates the conversion of the prochiral (*R*)-acetate group to (2*R*,3*S*)-(+)-isocitric acid (Figure 1). The body of evidence indicates that the general enzyme chemistry is essentially acid–base chemistry and not redox chemistry.

The discovery of the Fe–S cluster in aconitase provokes comment because the presence of similar clusters is usually associated with oxidation–reduction processes. A number of mechanistic proposals involving Fe(II) at the active center have been proffered to accommodate the results described above.[2-4] The proposals have in common the notion that a coordinated OH^- ion adds at the olefin to generate either citric or isocitric acid. If this proposal is valid, there is a prospect of observing such additions in model systems where OH^- is bound to a metal ion in near-neutral conditions especially when a carboxyl group attached to the olefin is also bound to the metal ion to give an intramolecular cyclization. Such models might also indicate the degree of increased reactivity toward hydration to be expected by organizing the reaction path in this way, the regiospecificity in such a process, i.e., whether there is a preference for five- or six-membered chelate formation, and what electronic factors, if any, govern the cyclization. There

(1) March, J. "Advanced Organic Chemistry: Reactions, Mechanisms and Structure", 2nd ed.; McGraw-Hill Kogakusha Ltd.: New York, 1977; p 696.
(2) Glusker, J. P. "The Enzymes"; Boyer, P. D., Ed.; Academic Press: New York, 1971; p 413.
(3) Kent, T. A.; Dreyer, J. L.; Kennedy, M. C.; Huynh, B. H.; Emptage, M. H.; Beinert, H.; Munck, E. *Proc. Natl. Acad. Sci. U.S.A.* **1982**, *79*, 1096–1100 and references therein.
(4) Emptage, M. H.; Kent, T. A.; Kennedy, M. C.; Beinert, H.; Munck, E. *Proc. Natl. Acad. Sci. U.S.A.* **1983**, *80*, 4674–4678. Emptage, M. H.; Dreyer, J.-L.; Kennedy, M. C.; Beinert, H. *J. Biol. Chem.* **1983**, *258*, 11106–11111.
(5) Beinert, H.; Emptage, M. H.; Dreyer, J.-L.; Scott, R. A.; Hahn, J. E.; Hodgson, K. O.; Thomson, A. J. *Proc. Natl. Acad. Sci. U.S.A.* **1983**, *80*, 393–396.
(6) Kennedy, M. C.; Emptage, M. H.; Dreyer, J.-L.; Beinert, H. *J. Biol. Chem.* **1983**, *258*, 11098–11105.
(7) Johnson, M. K.; Czernuszewicz, R. S.; Spiro, T. G.; Ramsay, R. R.; Singer, T. P. *J. Biol. Chem.* **1983**, *258*, 12771–12774.
(8) Villafranca, J. J.; Mildvan, A. S. *J. Biol. Chem.* **1971**, *246*, 772–779. Villafranca, J. J.; Mildvan, A. S. *J. Biol. Chem.* **1972**, *247*, 3454–3463. One referee has pointed out that these results could be due to adventiously bound iron.
(9) However, the following reference implies that a structure is imminent: Robbins, A. H.; Stout, C. D.; Piszkiewicz, D.; Gawron, O.; Yoo, C.-S.; Wang, B.-C.; Sax, M. *J. Biol. Chem.* **1982**, *257*, 9061–9063.
(10) Englard, S. *J. Biol. Chem.* **1960**, *235*, 1510.
(11) Hanson, K. R.; Rose, I. A. *Proc. Natl. Acad. Sci. U.S.A.* **1967**, *50*, 981.
(12) Rose, I. A.; O'Connell, E. L. *J. Biol. Chem.* **1967**, *242*, 1870–1879.

0002-7863/85/1507-6231$01.50/0

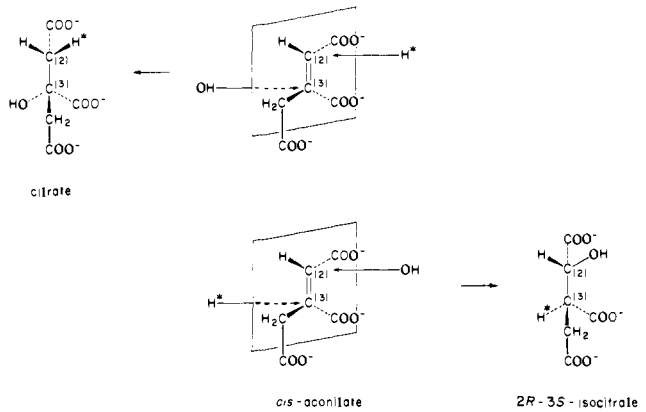

Figure 1. Isomerization of citric acid to isocitric acid through *cis*-aconitic acid, catalyzed by aconitic acid hydratase.

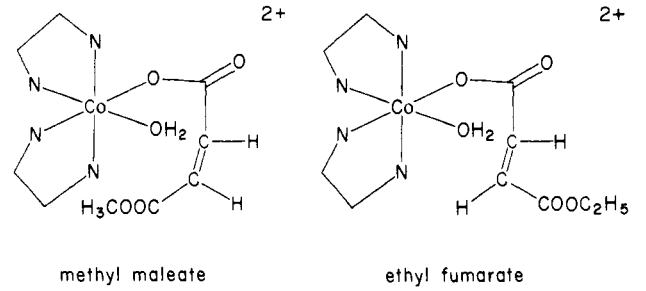

Figure 2. Methyl maleate and ethyl fumarate ions bound to aquabis(1,2-ethanediamine)cobalt(III).

are also stereochemical and reactivity aspects inherent in the chemistry which are interesting in their own right. This paper examines these questions by using some simple carboxylatoalkene systems bound to a bis(1,2-ethanediamine)cobalt(III) moiety cis to a coordinated water molecule (Figure 2). These complexes can be viewed simply as a metal ion holding the substrate and coordinated nucleophile close to one another under conditions where the coordinated OH^- ion has a near-maximum basicity for the neutral conditions required for it to act as a nucleophile in maximum concentration. The metal ion can be considered innocent in other respects. There is a precedent for such chemistry in the slow hydration of hydrogen maleate ion coordinated to a $Cr^{III}(H_2O)_5^{3+}$ center, leading to both chelated [(malato)tetraaqua]chromium(III) and [(fumarato)pentaaqua]chromium(III) ions.[13] In many respects, the Co(III) complexes are more tractable than those of Cr(III), and the current study allows a more detailed analysis of the reaction paths.

Experimental Section

Spectrophotometric rate data and visible spectra were collected by using Cary 16K and 118C recording spectrophotometers. The ^1H NMR spectra were recorded at 100 MHz by using a Jeol Model JNM-MH-100 minimar spectrometer with sodium 4,4-dimethyl-4-sila-1-pentanesulfonate (DSS) as internal reference. ^{13}C NMR spectra were recorded by using a Jeol FX60 spectrometer in the FT mode and 1,4-dioxane as an internal reference (δ 66.4 relative to tetramethylsilane). The NMR signals are recorded in parts per million (δ) positive downfield from the standards. All pH measurements were carried out with a Radiometer meter PHM26 fitted with a G202B glass electrode and a K4112 saturated calomel electrode connected via a 1.6 M NH_4NO_3, 0.2 M $NaNO_3$ salt bridge to minimize junction potentials. The pH equipment was calibrated with borate and phosphate buffers. All evaporations were carried out with Buchi evaporators under reduced pressure (~20 torr) so the temperature of the solution remained <25 °C.

Sodium Methyl Maleate. Maleic anhydride (18.6 g) dissolved in warm methanol (50 mL) was treated with sodium methoxide (10.8 g) slowly while the mixture was cooled on ice. After 1 h, the sodium methyl maleate was precipitated with ether (2 L) as a white oil which slowly crystallized. The crude product was recrystallized from methanol (50 mL) with diethyl ether, collected, and dried in vacuo (>90%). Anal. Calcd for $C_5H_5O_4Na$: C, 39.49; H, 3.31. Found: C, 39.0; H, 3.4. ^1H NMR (D_2O) δ 3.60 (s, 3 protons), 5.62 (d, 1 proton, $J \sim 12$ Hz), 6.39 (d, 1 proton, $J \sim 12$ Hz). Sodium *tert*-butyl maleate was prepared by an analogous route.

Sodium Ethyl Fumarate. Ethylfumaric acid (EGA) (14.4 g) suspended in water (25 mL) was neutralized with Na_2CO_3 (5.3 g). Ethanol and diethyl ether precipitated the salt as fine white crystals (>90%): ^1H NMR (D_2O) δ 1.28 (t, 3 protons), 4.26 (q, 2 protons), 6.46 (d, 1 proton, $J \sim 16$ Hz), 6.90 (d, 1 proton, $J \sim 16$ Hz).

***cis*-[Bis(1,2-ethanediamine)bis(methylmaleato)]cobalt(III) Perchlorate.** *cis*-$[Co(en)_2(Me_2SO)_2](ClO_4)_3$[14] (6.34 g) was refluxed in acetone (100 mL) with sodium methyl maleate (3.04 g) in methanol (20 mL) for 1 h. The solution was concentrated under reduced pressure and slowly added to ether (2 L). The crude product was collected, washed with ether, dissolved in the minimum volume of water at 80 °C, cooled in ice, and treated with $NaClO_4$. The red-violet crystals which separated were recrystallized from a minimum of hot water on cooling, washed with ethanol, and dried in vacuo over $Mg(ClO_4)_2$ (25%). Anal. Calcd for $C_{14}H_{26}N_4CoClO_{12}$: C, 31.39; H, 4.89; N, 10.44. Found: C, 31.0; H, 4.9; N, 10.4. ^1H NMR (D_2O) δ 2.60 and 2.90 (br structured peaks, CH_2), 3.74 (s, CH_3, 3 protons), 5.96 and 6.52 (d pair, CH=CH, $J \sim 12$ Hz, 4 protons), 4.1, 5.3, 5.7, 6.2 (br, $4NH_2$, 8 protons); ^{13}C NMR (D_2O) 43.5 and 44.9 (CH_2CH_2), 52.1 (CH_3), 121.0 and 138.0 (CH=CH), 167.6 and 178.1 (C=O).

***cis*-[Bis(1,2-ethanediamine)(dimethyl sulfoxide)(ethylfumarato)]cobalt(III) Perchlorate.** Sodium ethyl fumarate (1.9 g) was added to *cis*-$[(en)_2Co(Me_2SO)_2](ClO_4)_3$ (7.0 g) in dry Me_2SO (50 mL) and the mixture heated on a steam bath for 40 min. After cooling, the solution was slowly stirred into an ethanol–ether mixture (1:9, 1 L), and the gum obtained was triturated with ether until solid. The crude product was dissolved in a minimal amount of water and crystallized by adding $NaClO_4$. The crystals were washed with a little ice–water and dried in vacuo over P_2O_5. Anal. Calcd for $CoC_{12}H_{29}C_4SCl_2O_{13}\cdot H_2O$: Co, 9.55; C, 23.35; H, 5.06; N, 9.08. Found: Co, 9.5; C, 23.6; H, 4.8; N, 9.1. ^1H NMR (D_2O) δ 1.30 (t, CH_3, 3 protons), 2.8 (d, Me_2SO), 4.2 (q, CH_2), 2.4 and 3.9 (br structured peaks, CH_2), 4.2 and 5.8 (br, $4NH_2$, 8 protons), 6.5 and 6.75 (d pair, CH=CH, $J \sim 16$ Hz, 2 protons).

Bis(1,2-ethanediamine)cobalt(III) Methylmalato Isomers. $[Co(en)_2(OH)(OH_2)](ClO_4)_2$[15] (16.5 g) was treated with sodium methyl maleate (6.1 g) in water (30 mL) and stirred for 3 days at 25 °C. The solution, acidified to pH 3 with $HClO_4$, was cooled in ice. Pink crystals were collected, washed with methanol, and dried in air. Addition of more $HClO_4$ and $NaClO_4$ and cooling gave three more fractions. Fractions 1 and 2 were recrystallized together to give the less-soluble isomer. Anal. Calcd for $CoC_9H_{22}N_4O_{13}Cl_2$: C, 20.62; H, 4.23; N, 10.69. Found: C, 20.4; H, 4.5; N, 10.5. Fractions 3 and 4 were recrystallized together to remove the less-soluble component and finally gave the most soluble isomer. Anal. Calcd for $CoC_9H_{22}N_4O_{13}Cl_2\cdot H_2O$: C, 19.94; H, 4.46; N, 10.33. Found: C, 19.7; H, 4.4; N, 10.2. The bromide salts of the diastereoisomers were isolated similarly. Anal. Calcd for (less-soluble isomer) $CoC_9H_{22}N_4O_5Br_2\cdot 2H_2O$: C, 20.74; H, 5.04; N, 10.75. Found: C, 20.5; H, 4.80; N, 10.4. Anal. Calcd for (more-soluble isomer) $CoC_9H_{22}N_4O_5Br_2\cdot 2H_2O$: C, 20.74; H, 5.04; N, 10.75. Found: C, 20.99; H, 4.65; N, 10.79. ^1H NMR (D_2O perchlorate salt less-soluble isomer) δ 2.81 (m, $(CH_2)_2$), 2.96 (d, CH_2), 3.72 (s, CH_3), 4.54 (t, CH), 5.63 (m, NH); ^{13}C NMR (D_2O) δ 37.5, 43.1, 43.5, 45.4 (CH_2), 52.6 (CH_3), 71.3 (CH), 173.3 and 183.7 (C=O); ^1H NMR (D_2O perchlorate salt more soluble isomer) δ 2.84 (m, $(CH_2)_2$), 2.96 (d, CH_2), 3.73 (s, CH_3), 4.51 (t, CH), 5.48 (m, NH); ^{13}C NMR (D_2O) δ 37.3, 42.7, 44.3, 45.6, 46.0 (CH_2), 52.6 (CH_3), 70.8 (CH), 173.2 and 183.3 (C=O).

***trans*-[Bis(1,2-ethanediamine)bis(ethylfumarato)]cobalt(III) Perchlorate.** Fumaric acid monoethyl ester (0.72 g) and *cis*-$[Co(en)_2(OH)(OH_2)](ClO_4)_2$[15] (2.1 g) were mixed in water (40 mL) and heated on a steam bath for 2 h. The solution deposited mauve-pink crystals on cooling which were sparingly soluble in water. Anal. Calcd for $CoC_{16}H_{30}N_4O_{12}Cl\cdot H_2O$: C, 32.97; H, 5.53; N, 9.61. Found: C, 32.1; H, 5.6; N, 9.7. ^1H NMR (acetone-d_6) δ 1.3 (t, CH_3), 3.0 (s, CH_2), 4.3 (q, ester CH_2), 6.2 (br, s, NH_2), 6.6 (s, CH=CH). A similar spectrum was obtained in Me_2SO-d_6.

***trans*-[Bis(1,3-propanediamine)bis(ethylfumarato)]cobalt(III) Perchlorate.** This compound was synthesized by using *trans*-$[Co(tn)_2(OH)(OH_2)](ClO_4)_2$[16] by a method analogous to that above except that the heating period was 5 min and $NaClO_4$ was added to crystallize the complex. Anal. Calcd for $CoC_{18}H_{34}N_4O_{12}Cl$: C, 36.47; H, 5.78; N,

(13) Olsen, M. V.; Taube, H. *J. Am. Chem. Soc.* **1970**, *92*, 3236–3237.

(14) Jackson, W. G.; Sargeson, A. M. *Inorg. Chem.* **1978**, *17*, 1348–1362.
(15) Kruse, W.; Taube, H. *J. Am. Chem. Soc.* **1961**, *83*, 1280–1284.
(16) Jonasson, I. R.; Lincoln, S. F.; Stranks, D. R. *Aust. J. Chem.* **1970**, *23*, 2267–2278.

9.45. Found: C, 36.5; H, 5.8; N, 9.2. ^{1}H NMR (acetone-d_6) δ 1.3 (t, CH_3), 2.7 (quintet, CH_2–tn), 2.9 (s, CH_2–tn central), 4.3 (q, ester CH_2), 5.8 (br, s, NH_2), 6.6 (d, pair CH=CH, J = 12 Hz).

***cis*-[Bis(1,2-ethanediamine)bis(*tert*-butylmaleato)]cobalt(III) Perchlorate Dihydrate.** Sodium *tert*-butyl maleate (3.6 g) and *cis*-[Co(en)$_2$(Me$_2$SO)$_2$](ClO$_4$)$_3$ (9.0 g) were refluxed in dry acetone (250 mL) for 30 min. After filtration the solution was concentrated to 50 mL and added dropwise to vigorously stirred ether (500 mL). The oil was collected, redissolved in acetone and the procedure repeated twice more. The mauve powder finally obtained was recrystallized by adding hot water (70 °C) and cooling the filtrate rapidly in ice. Addition of $NaClO_4$ also assists the precipitation of the complex which was washed with a little ice-water and dried in vacuo. Anal. Calcd for $C_{20}H_{28}N_4O_{12}ClCo\cdot 2H_2O$: C, 36.56; H, 6.44; N, 8.53. Found: C, 36.5; H, 6.2; N, 8.6. ^{1}H NMR (Me$_2$SO-d_6) δ 1.45 (s, CH_3), 2.55 and 2.8 (br, s, CH_2–CH_2), 4.3, 5.5, 6.45 (br, s, NH_2), 6.0 and 6.65 (d, pair CH=CH).

Hydration of Alkenic Substrates by *cis*-[Co(tn)$_2$(OH)(OH$_2$)](ClO$_4$)$_2$. Sodium methyl maleate, sodium ethyl fumarate, sodium 3-chloropropenoate, sodium 2-chloropropenoate, or sodium propenoate (10^{-4} mol) was dissolved in D_2O (0.5 mL) and treated with the hydroxoaqua complex[16] (10^{-4} mol). The ^{1}H NMR spectra were measured at appropriate intervals (see Figure 8) and the solutions were maintained at 30 °C during and between scans.

Spectrophotometric Kinetic Measurements. Solutions of the *cis*-[Co(en)$_2$(OH$_2$)(methylmaleato)]$^{2+}$ ion were prepared by dissolving *cis*-[Co(en)$_2$(methylmaleato)$_2$](ClO$_4$) (1.134 g) in water (25 mL) and adding 0.2 M $HClO_4$ (25 mL) at μ = 0.2 or 1.0 ($NaCF_3SO_3$ or $NaClO_4$) as required. The solutions were maintained at 25 °C for 4 h ($10t_{1/2}$ for aquation).

(a) pH Stat. All reactions were followed at 25.00 ± 0.05 °C while maintaining the desired pH with a Radiometer pH-Stat. The pH of a solution of the *cis*-[Co(en)$_2$(OH$_2$)(methylmaleato)]$^{2+}$ ion in 0.1 M $HClO_4$ (μ = 0.1 M $NaCF_3SO_3$ or $NaClO_4$) was adjusted to the desired value with 2 M NaOH, and the rate of cyclization was followed spectrophotometrically at 356 nm.

(b) Stopped Flow. Solutions of the *cis*-[Co(en)$_2$(OH$_2$)(methylmaleato)]$^{2+}$ ion in 0.1 M $HClO_4$ (μ = 1.0 M $NaCF_3SO_3$ or $NaClO_4$) (9 mL) were mixed with a solution containing 0.1 M NaOH (μ = 1.0 M $NaCF_3SO_3$ or $NaClO_4$) (9 mL) and the appropriate buffer solution (μ = 1.0 M $NaCF_3SO_3$ or $NaClO_4$) (19.5 mL).

The mixing was carried out in a stopped-flow reactor with three reservoirs where the complex solution and base were mixed first and then with the buffer. The absorbance change was followed at 356 nm by using a 5-cm cell. Reactions were followed for at least 10 half-lives, and plots of log ($A_\infty - A$) vs. time were linear for at least three half-lives. For the reactions where products were isolated, μ = 0.2 M throughout ($NaCF_3SO_3$ or $NaClO_4$). The solutions were collected, and the pH was checked against the initial buffer mixture and found to be unchanged (±0.01 pH units). All rate constants quoted are an average of at least two determinations with a maximum deviation of 4%.

After quenching to pH 3 with acetic acid and after dilution, the mixture was absorbed on Sephadex C25 cation-exchange resin (Na^+ form). After washing with water, the products were separated by elution from the column by using sodium acetate–acetic acid buffer (0.1 M), pH 4.4. The cobalt content was determined by atomic absorption spectroscopy.

A similar procedure was employed to study the reactions of the *cis*-[Co(en)$_2$(OH$_2$)(ethylfumarato)]$^{2+}$ complex.

The products from these reactions were identified after chromatography of the reaction mixtures on Sephadex C25 cation-exchange resin. Elution with acetate buffer (0.1 M, pH 4) separated 1+ and 2+ cationic components. The 1+ band was identified as chelated methylmalato from comparisons of the spectral properties with an authentic sample. The 2+ band, after collection, was sorbed on Dowex 50 WX2 cation-exchange resin and, after washing, was eluted with 3 M HCl. The acid solution was rotary-evaporated to dryness 3 times and then reevaporated with D_2O. The ^{1}H NMR spectrum of the residue was consistent with the presence of ethyl fumarate.

pK_a Determination. The pK_a of the *cis*-[Co(en)$_2$(OH$_2$)(methylmaleato)]$^{2+}$ ion was determined by using the initial absorbance method[17] with 0.05 M imidazole buffers (1 M $NaClO_4$). A solution of the *cis*-[Co(en)$_2$(OH$_2$)(methylmaleato)]$^{2+}$ ion was prepared by acid hydrolysis of the bis(maleato) complex as described and isolated after chromatography on Sephadex C25 cation-exchange resin and elution with 0.2 M $NaClO_4$ solution. The ionic strength of the final solution was adjusted by using $NaClO_4$ (μ = 1.0 M). The solutions of the aqua complex and appropriate buffer were mixed rapidly in a manually operated stopped-flow device. The initial absorbance after mixing (~1 s) was measured at 540 nm. Measurements covered the pH range 4.64–7.72 and the pK_a evaluated from the absorbance changes was 7.14 at 25 °C, μ = 1.0 M ($NaClO_4$).

The pK_a of the least-soluble chelated malate diastereoisomer was determined as follows: 0.26258 g of complex (5×10^{-4} mol) was dissolved in 50 cm^3 of H_2O and the ionic strength adjusted to μ = 1.0 M with $NaNO_3$. The complex was titrated with 1 M NaOH in 0.05-cm^3 aliquots from a micrometer syringe. The pH of the solution was monitored by using a Radiometer PHM 26 and a K4112 saturated calomel electrode connected through a 1.6 M NH_4NO_3, 0.2 M $NaNO_3$ salt bridge. The pK_a was calculated as 2.75 ± 0.03 by using the previously described method.[18]

Deuteration Studies. The bis(methylmaleato) complex was hydrolyzed, as previously described, by using a 0.1 M $DClO_4$–D_2O solution and the chelated maleate complex prepared by reaction in deuterated buffer–D_2O solution (pH 8.0 imidazole–$DClO_4$, 0.02 M) or NaOD (pH 13). In each case, the reaction was quenched, after $10t_{1/2}$, with $DClO_4$. The malate complex was isolated, after chromatography on Sephadex C25 cation-exchange resin (Na^+ form) using acetate buffer 0.1 M (pH 4.4) as eluent. The less-soluble diastereoisomer was crystallized as its perchlorate salt from the mixture eluted from the column, after volume reduction and addition of solid $LiClO_4$. The ^{1}H NMR spectra were recorded by using a Bruker CXP 200-MHz spectrometer with Me$_2$SO-d_b as the solvent.

^{18}O-Labeling Experiments. Labeled *cis*-[Co(en)$_2$(^{18}OH$_2$)(methylmaleato)]$^{2+}$ ion was obtained after dissolving *cis*-[Co(en)$_2$(methylmaleato)$_2$](ClO$_4$) (0.4 g) in 0.1 M CF_3SO_3H $^{18}OH_2$ (10% enriched) solution (10 mL) and allowing the acid hydrolysis to proceed for $10t_{1/2}$. The pH of the solution was adjusted to 3 with NaOH solution (2 M) and the labeled water was removed by freeze-drying under vacuum (<10^{-3} mmHg). The residue of complex was dissolved in water (3 mL), and the pH of the solution was adjusted to 12 with NaOH solution (2 M). The reaction was quenched after $10t_{1/2}$ with concentrated $HClO_4$. Solid $NaClO_4$ was added to crystallize the complex perchlorate which was then converted to the bromide form by using Sephadex C25 cation-exchange resin with 0.1 M LiBr solution as eluant. The complex bromide was heated to 290 °C in the direct-inlet probe of a MS9 mass spectrometer whence the methyl malate ligand distilled off the metal ion. The peak heights at mass numbers 89, 91, 99, 101, 103, 105 and 117, and 119 were measured. The mass spectrum of the complex prepared in an analogous manner from unlabeled water was also recorded under the same conditions.

Collection and Reduction of X-ray Intensity Data. Approximate unit cell dimensions for crystals of $\Delta(S),\Lambda(R)$-[Co(en)$_2$(methylmalato)]-$Br_2\cdot 2H_2O$ were obtained from preliminary Weissenberg ($hk0$, hkl) data and precession ($0kl$, $1kl$, $h0l$, $h1l$ data) photographs which showed systematic absences (hkl data, $h + k = 2n + 1$; $h0l$ data, $l = 2n + 1$) corresponding to the *C*-centered space groups *Cc* (*Cs*^{4}, no. 9) or *C*2/*c* (*C*2*h*6, no. 15). The choice of the acentric space group, *Cc*, has been confirmed by the successful solution and refinement of the structure.

Accurate unit cell dimensions, together with estimated standard errors, and the crystal orientation matrix, were obtained in the usual way[19] from the least-squares refinement of the 2θ, ω, χ, ϕ values found for 12 carefully centered reflections with $2\theta > 74°$. Full details of crystal data are given in Table I in the supplementary material.

Data were collected by using a Picker FACS-I fully automatic diffractometer; collection details and experimental conditions used are given in Table II in the supplementary material.

During data collection, the intensities of each of the three standard reflections decreased by more than 20%. Crystal decomposition was assumed to be anisotropic but independent of 2θ. Before further calculation, the intensity data were corrected for decomposition effects. Reflection intensities were reduced to values of $|F_o|$, and each was assigned an individual estimated standard deviation.[20] For this data set, the

(17) Albert, A.; Serjeant, E. P. "The Determination of Ionization Constants: A Laboratory Manual", 2nd ed.; Chapman and Hall: London, 1971; p 44.

(18) Reference 17, p 27.

(19) The programs contained in the Picker Corps FACS-I Disk Operating System (1972) were used for all phases of diffractometer control and data collection.

(20) The formulas used for data reduction are as follows: LP (Lorentz polarization factor) = $(\cos^2 2\theta + \cos^2 2\theta_m)/2 \sin 2\theta$ where θ and θ_m (=13.25°) are the reflection and monochromator Bragg angles, respectively; I (net peak intensity) = $[C_T - (t_p/t_b)(B_1 + B_2)]$ where C_T is the total peak count in t_p (seconds and B_1 and B_2 are the individual background counts in $(t_b/2)$ (seconds); $\sigma(I)$ (reflection significance) = $[C_T + (t_p/t_b)^2/(B_1 + B_2)]^{1/2}$; $\sigma(F_o)$ (the reflection esd) = $\{[\sigma(I)/\mathrm{LP})^2 + (p|F_o|^2)^2\}^{1/2}/2|F_o|$; $\sigma_s(F_o)$ (the reflection esd from counting statistics alone) = $\sigma(I)/2(\mathrm{LP})(|F_o|)$; R_s (the statistical R factor) = $\sum\sigma_s(F_o)/\sum|F_o|$; background rejection ratio $(|B_1 - B_2|)/(B_1 + B_2)^{1/2} \geq 3.0$.

Table V. Atomic Coordinates for $[(en)_2Co(methylmalato)]Br_2 \cdot 2H_2O$

atom	X/A	Y/B	Z/C
Co	0.39975 (36)	0.58923 (10)	0.38135 (33)
O(1)	0.3419 (10)	0.5437 (4)	0.4885 (10)
O(2)	0.3006 (11)	0.5142 (4)	0.2364 (11)
N(1)	0.4684 (13)	0.6293 (5)	0.2739 (12)
N(2)	0.5917 (14)	0.5387 (5)	0.4986 (14)
N(3)	0.2064 (13)	0.6415 (5)	0.2604 (13)
N(4)	0.4860 (13)	0.6603 (5)	0.5369 (12)
C(1)	0.2529 (15)	0.4941 (6)	0.4165 (16)
C(2)	0.1956 (17)	0.4871 (7)	0.2489 (16)
C(3)	0.6248 (23)	0.6086 (10)	0.3462 (25)
C(4)	0.6586 (29)	0.5463 (13)	0.4173 (36)
C(5)	0.2357 (15)	0.7074 (6)	0.3299 (17)
C(6)	0.3578 (18)	0.6983 (8)	0.5095 (18)
O(11)	0.2002 (12)	0.4590 (4)	0.4656 (11)
C(21)	0.1946 (18)	0.4043 (7)	0.2218 (17)
C(22)	0.3470 (20)	0.3710 (7)	0.3504 (21)
O(22)	0.4530 (14)	0.3958 (5)	0.4741 (16)
O(23)	0.3495 (16)	0.3053 (6)	0.3190 (15)
C(24)	0.4808 (26)	0.2659 (9)	0.4491 (28)
Br(1)	0.60404	0.78667 (8)	0.42565
Br(2)	0.91288 (34)	0.58860 (9)	0.25486 (32)
OW(1)	0.1961 (16)	0.1209 (8)	0.8770 (15)
OW(2)	0.3855 (16)	0.0766 (9)	0.8232 (21)

instrumental "uncertainty" factor (ρ)[21,22] was assigned a value of $0.002^{1/2}$. The reflection data were sorted into a convenient order, equivalent reflection forms were averaged, and those reflections for which $I/\sigma(I) \leq 3.0$ were discarded as being unobserved.[20] Reflections for which the individual background measurements differed by more than 4.0σ were also rejected. The statistical R factor[20] (R_s) for the 1628 reflections of the terminal data set was 0.027.

Solution and Refinement of the Structure. A statistical analysis of the normalized structure factors gave values of 0.769 for average $|E^2 - 1|$ and 0.865 for average $|E|$, suggesting that the structure was probably acentric [the theoretical values for these quantities are average $|E^2 - 1|$, 0.968 (centric), 0.736 (acentric) and average $|E|$, 0.798 (centric), 0.886 (acentric)].[23] The structure was solved by using the MULTAN package, and 32 sets of signs were determined for the 300 reflections with $|E| > 1.31$. The starting set chosen is given in Table III in the supplementary material, and the subsequent E map showed the positions of the two bromine atoms, the cobalt atom, and the oxygen and nitrogen atoms of the first coordination sphere. The remaining atoms of the molecule were located from successive difference Fourier syntheses. When data which had been corrected for absorption effects[24] were used, the structure was refined by block diagonal and (finally) full-matrix least-squares methods to unweighted and weighted R factors of 0.054 (R) and 0.059 (R_w), respectively. Atomic scattering factors for the nonhydrogen atoms were taken from the compilation of Cromer and Mann[25] and were corrected for the real and imaginary parts of anomalous scattering.[26,27] Hydrogen atom scattering factors were taken from the compilation of Stewart et al.[28] A full account of the course of refinement is given in Table IV in the supplementary material.

Calculated hydrogen atom coordinates [assuming N–H = 0.87 Å, C–H = 0.95 Å, $B_H = 1.1B_C$ (or $1.1B_N$) O^2] were included as fixed contributions to F_c in the final refinement cycles and were recalculated prior to each refinement cycle. No attempt was made to include the methyl [C(24)], hydroxyl [O(2)], or solvent molecule [OW(1) and OW(2)] hydrogen atoms in the scattering model.

On the final cycle of least-squares refinement, no individual parameter shift was greater than 0.07 of the corresponding parameter estimated standard deviation. A final electron-density difference map showed no unusual features, and there were no residual peaks greater than 0.8 e/Å^3 (less than one-fifth the height of typical carbon atom peaks on earlier difference maps). The standard deviation of an observation of unit weight, defined as $[\sum\omega(|F_o| - |F_c|)^2/(m-n)]^{1/2}$ [where m is the number of observations, and n (=206) is the number of parameters varied] is 1.85, cf. an expected value of 1.0 for ideal weighting. There was no evidence of serious extinction effects, and no correction was applied. There were no serious trends in the dependence of the minimized function on $|F_o|$, $\lambda^{-1} \sin\theta$, or Miller index.

The atomic coordinates for $[Co(en)_2(methylmalato)]Br_2 \cdot 2H_2O$ together with their estimated standard deviations (where appropriate) are listed in Table V. A listing of observed and calculated structure factor amplitudes [x10 (electrons)] is available (for details regarding the availability of supplementary material, see the paragraph at the end of this paper).

The crystal structure is noncentrosymmetric, and the "handedness" of the molecule was established at refinement set 1 of Table IV. For the molecule of correct configuration, the unweighted and weighted R factors were 0.137 and 0.157, respectively, while the standard deviation of an observation of unit weight (see above) was 12.8. For the "incorrect" molecule (i.e., of inverse configuration), the corresponding values were 0.175, 0.194, and 15.8, respectively.

All calculations were carried out on the Univac 1108 computer at The Australian National University Computer Center by using the ANUCRYS suite of crystallographic programs which are fully detailed in ref 29.

Results

Syntheses and Reactivity. *cis*-$[Co(en)_2(methylmaleato)_2]ClO_4$ was synthesized from the *cis*-$[Co(en)_2(Me_2SO)_2](ClO_4)_3$ complex and the methyl maleate ion in acetone. The stereochemistry of the complex was assigned as cis from the ^1H NMR spectrum in D_2O solution where four broad N–H signals were observed. The symmetry of the trans isomer generates only one N–H signal. *cis*-$[Co(en)_2(ethylfumarato)(Me_2SO)](ClO_4)_2$ was synthesized from the bis(Me_2SO) complex and the ethylfumarate ion in dimethyl sulfoxide solution. The cis configuration was established from the doublet observed at δ 2.8 for the diastereotopic methyl groups in the oxygen-bound Me_2SO. In the trans isomer, both methyl groups are equivalent.

The *trans*-$[Co(en)_2(ethylfumarato)_2]ClO_4$ complex was prepared from the reaction between *cis*-$[Co(en)_2(OH)(OH_2)](ClO_4)_2$ and the monoethyl ester of fumaric acid in aqueous solution. The analogous *trans*-$[Co(tn)_2(ethylfumarato)_2]^+$ complex was prepared from the *trans*-$[Co(tn)_2(OH)(OH_2)](ClO_4)_2$ complex as above. *cis*-$[Co(en)_2(tert\text{-}butylmaleato)_2]ClO_4$ complex was prepared from the reaction between *cis*-$[Co(en)_2(Me_2SO)_2](ClO_4)_3$ and sodium *tert*-butyl maleate in acetone.

The *cis*-$[Co(en)_2(methylmaleato)_2]^+$ complex was found to lose one methylmaleato ion by an acid-catalyzed path with a half-life of approximately 22 min at 30 °C in 0.1 M DCl. The aquation took place almost exclusively with retention of the cis configuration as evidenced by ^1H NMR spectroscopy which showed the disappearance of the doublet pairs due to the reactant and the appearance of the doublet pair due to free methyl maleic acid at δ 6.38, 6.48, 6.54, and 6.6. The spectrum then remained unchanged over $6t_{1/2}$ or more, indicating that the isomerization to the trans isomer was slow by comparison to aquation in the acid solution. The aquamaleato complex also exhibited a complex set of N–H signals in the ^1H NMR spectrum consistent with a cis configuration.

The pattern for the aquation of *cis*-$[Co(en)_2(methylmaleato)_2]^+$ and isomerization of *cis*-$[Co(en)_2(OH_2)(methylmaleato)]^{2+}$ complexes were also consistent with that observed for the aquation of the diacetato complex ion, *cis*-$[Co(en)_2(CH_3COO)_2]^+$ where $k_{aq} = 5.4 \times 10^{-2}$ s^{-1}, $[H^+] = 0.1$ M at 30 °C, and for the isomerization of the aquaacetato product *cis*-$[Co(en)_2(OH_2)(CH_3COO)]^{2+}$, k_i ($=k_{ct} + k_{tc}$) $= 5.7 \times 10^{-5}$ s^{-1} at 30 °C.[30] The latter reaction was found to be independent of acid from 0.01 to 1.0 M $[H^+]$.[30] Repeated attempts to crystallize the *cis*-$[Co(en)_2(OH_2)(methylmaleato)]^{2+}$ complex were unsuccessful.

(21) Busing, W. R.; Levy, H. A. *J. Chem. Phys.* **1957**, *26*, 563–568.
(22) Corfield, P. W. R.; Doedens, R. J.; Ibers, J. A. *Inorg. Chem.* **1967**, *6*, 197–204.
(23) Karle, I. L.; Dragonette, K. S.; Brenner, S. A. *Acta Crystallogr.* **1965**, *19*, 713–716.
(24) The crystal chosen for data collection was bounded by the faces {110}, {1$\bar{1}$0}, {0$\bar{1}$0}, {010}, {111}, and {1$\bar{1}$1}. The perpendicular distances between these faces were {110} to {1$\bar{1}$0}, 0.014 cm, {0$\bar{1}$0} to {010}, 0.009 cm, {111} to {1$\bar{1}$1}, 0.027 cm. The transmission factor, applied to $|F_o|$, ranged from 0.389 to 0.658.
(25) Cromer, D. T.; Mann, J. B. *Acta Crystallogr.* **1968**, *A24*, 321–324.
(26) Prewitt, C. T. Ph.D. Thesis, Massachusetts Institute of Technology, 1962, p 163.
(27) Cromer, D. T.; Liberman, D. *J. Chem. Phys.* **1970**, *53*, 1891–1898.
(28) Stewart, R. F.; Davidson, E. R.; Simpson, W. T. *J. Chem. Phys.* **1965**, *42*, 3175–3187.
(29) Ferguson, J.; Mau, A. W.-H.; Whimp, P. O. *J. Am. Chem. Soc.* **1979**, *101*, 2363–2369.
(30) Dasgupta, T. P.; Tobe, M. L. *Inorg. Chem.* **1972**, *11*, 1011–1016.

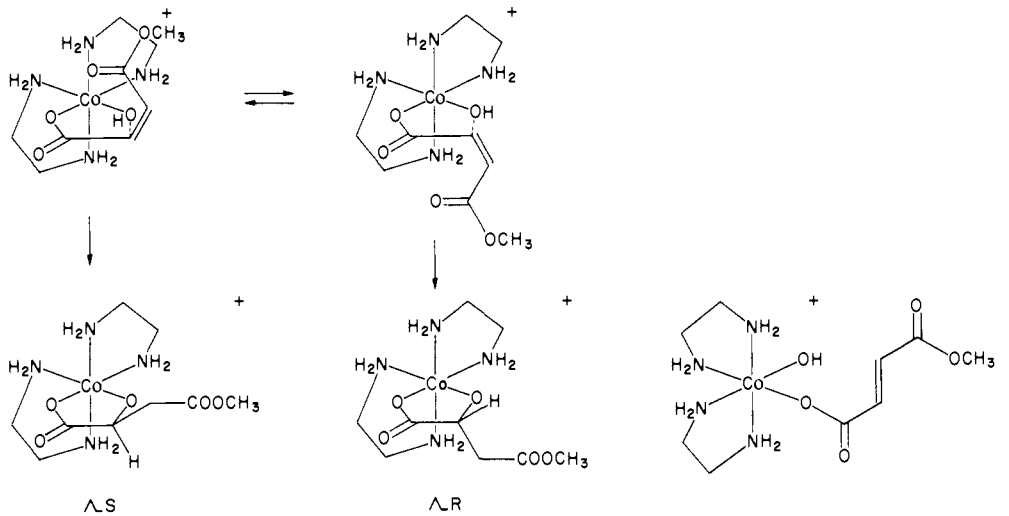

Figure 3. Products of the cyclization of *cis*-$[Co(en)_2(OH)(methylmaleato)]^{2+}$ ion under pH-stat conditions.

Table VI. Bond Distances and Interbond Angles

(a) Bond Distances, Å

atoms	distance	atoms	distance	atoms	distance
Co–O(1)	1.905 (8)	Co–O(2)	1.934 (8)	Co–N(1)	1.952 (10)
Co–N(2)	1.931 (2)	Co–N(3)	1.959 (11)	Co–N(4)	1.937 (11)
O(1)–C(1)	1.256 (14)	C(1)–O(11)	1.243 (14)	C(1)–C(2)	1.552 (19)
O(2)–C(2)	1.458 (15)	C(2)–C(21)	1.498 (18)	C(21)–C(22)	1.500 (21)
C(22)–O(22)	1.198 (16)	C(22)–O(23)	1.359 (18)	O(23)–C(24)	1.457 (20)
N(1)–C(3)	1.442 (20)	C(3)–C(4)	1.385 (27)	C(4)–N(2)	1.503 (24)
N(3)–C(5)	1.448 (16)	C(5)–C(6)	1.531 (20)	C(6)–N(4)	1.471 (18)

(b) Interbond Angles, deg

atoms	angle	atoms	angle	atoms	angle
O(1)–Co–O(2)	84.4 (4)	O(1)–Co–N(1)	175.3 (4)	O(1)–Co–N(2)	90.7 (4)
O(1)–Co–N(3)	90.5 (4)	O(1)–Co–N(4)	88.4 (4)	O(2)–Co–N(1)	93.1 (4)
O(2)–Co–N(2)	87.2 (4)	O(2)–Co–N(3)	93.0 (4)	O(2)–Co–N(4)	172.6 (4)
N(1)–Co–N(2)	85.2 (5)	N(1)–Co–N(3)	93.6 (4)	N(1)–Co–N(4)	94.2 (4)
N(2)–Co–N(3)	178.8 (5)	N(2)–Co–N(4)	94.7 (5)	N(3)–Co–N(4)	85.3 (5)
Co–O(1)–C(1)	115.4 (8)	Co–O(2)–C(2)	111.8 (7)	O(1)–C(1)–C(2)	117.9 (11)
O(1)–C(1)–O(11)	124.8 (13)	O(11)–C(1)–C(2)	117.2 (11)	O(2)–C(2)–C(1)	105.7 (10)
O(2)–C(2)–C(21)	111.6 (11)	C(1)–C(2)–C(21)	112.6 (11)	C(2)–C(21)–C(22)	112.7 (12)
C(21)–C(22)–O(22)	125.9 (13)	C(21)–C(22)–O(23)	112.5 (14)	O(22)–C(22)–O(23)	121.3 (15)
C(22)–O(23)–C(24)	116.2 (14)	Co–N(1)–C(3)	111.1 (9)	N(1)–C(3)–C(4)	111.2 (16)
C(3)–C(4)–N(2)	111.7 (18)	C(4)–N(2)–Co	108.4 (10)	Co–N(3)–C(5)	110.3 (9)
N(3)–C(5)–C(6)	106.7 (11)	C(5)–C(6)–N(4)	105.5 (11)	C(6)–N(4)–CO	109.2 (8)

Addition of base to solutions of the *cis*-$[Co(en)_2(OH_2)(methylmaleato)]^{2+}$ ion (pK_a = 7.14) generated the hydroxo complex and allowed an intramolecular cyclization to produce a chelated methylmalato ligand and the isomerized hydroxofumarato complex, Figure 3. The chelated methylmalate can exist in two diastereoisomeric forms, Figure 3. Both $[Co(en)_2(methylmalato)]^{2+}$ diastereoisomers were synthesized in other ways. Sodium methyl maleate and *cis*-$[Co(en)_2(OH)(OH_2)]^{2+}$ were reacted in water at room temperature for 3 days. The relatively rapid water exchange observed for the hydroxoaqua ion[15] allows the entry of the ligand followed by its cyclization with a bound hydroxide ion. The two diastereoisomers were isolated as bromide or perchlorate salts from aqueous solution. Their ^1H NMR spectra showed barely different singlets for the ester methyl groups, complex signals for the malate CH_2 group, which were well resolved, and well-separated triplets for the methine protons arising from coupling with the adjacent methylene moiety.

The Me_2SO in the $[Co(en)_2(Me_2SO)(methylmaleato)]ClO_4$ salt was also aquated in acid solution over ~30 min to give largely the *cis*-$[Co(en)_2(H_2O)(methylmaleato)]^{2+}$ ion. Addition of Na_2CO_3 generated the hydroxo ion, and this complex also rapidly cyclized to the methyl malate chelate.

To confirm the proposal of methyl malate chelation via either a five- or a six-membered ring, an X-ray crystallographic analysis of the less soluble diastereoisomeric bromide salt was carried out.

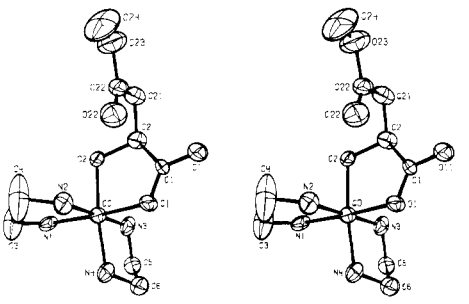

Figure 4. Perspective view of the stereochemistry of the molecule Δ-(*S*)-$[Co(en)_2(methylmalato)]Br_2 \cdot 2H_2O$.

Discussion of the Structure. Crystals of $[Co(en)_2(methylmalato)]Br_2 \cdot 2H_2O$ contain equal quantities of Δ-$[Co(en)_2(S)(methylmalato)]^{2+}$ and Λ-$[Co(en)_2(R)(methylmalato)]^{2+}$. In addition, there are two bromide ions and two solvent water molecules per cobalt atom. The complex cation has no imposed crystallographic symmetry. The coordination at the central cobalt atom is essentially octahedral, with four coordination sites being occupied by ethylenediamine groups. The two remaining sites are occupied by oxygen atoms of the methylmalato ligand. A perspective view of the molecule is shown by the stereopairs of Figure 4, while the contents of one unit cell are shown by the

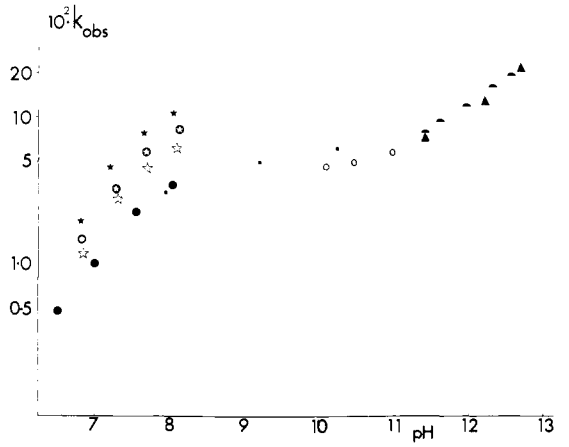

Figure 6. Rate profile for the cyclization of *cis*-[(1,2-ethanediamine)-Co(OH)(methylmaleato)]$^+$ at 25 °C, μ = 1.0 M ($NaClO_4$). (★) 0.2 M imidazole, ( ) 0.1 M imidazole, (☆) 0.05 M imidazole, (●) pH state, (▲) OH, (○) 0.05 M diethylamine, (■) 0.05 M diethanolamine, ( ) 0.05 M guanidine, (□) 0.1 M Tris.

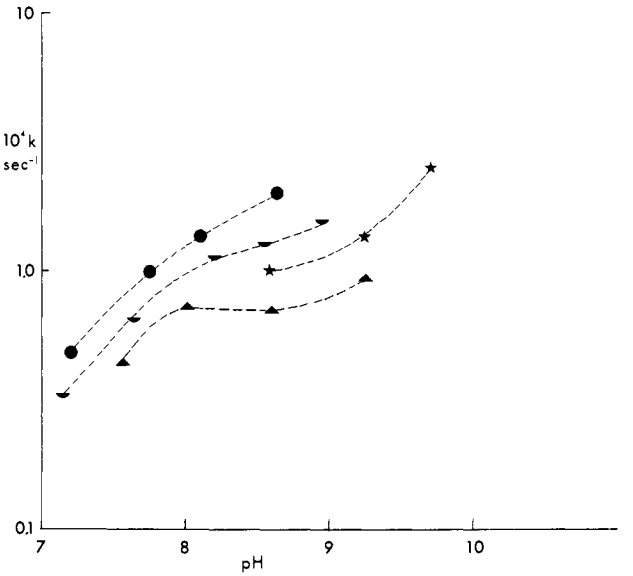

Figure 7. Rate profile for the cyclization of *cis*[(1,2-ethanediamine)-Co(OH)(ethylfurmarato)]$^+$ at 25 °C, μ = 1.0 M ($NaClO_4$). (●) 0.1 M Tris, ( ) 0.05 M Tris, (▲) pH stat, (★) 0.05 M diethanolamine.

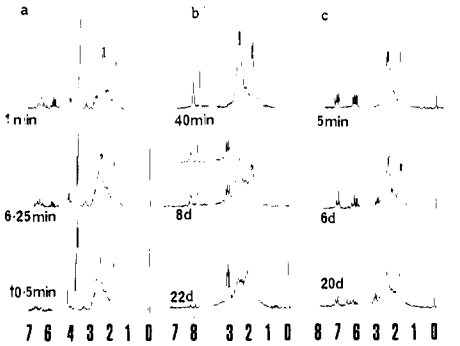

Figure 8. ^{1}H NMR spectra of the reaction of $[(tn)_2Co(OH)(OH_2)]^{2+}$ with sodium salts of (a) methyl maleate, (b) 2-chloropropenoate, and (c) *trans*-3-chloropropenoate (see Experimental Section for details).

stereopairs of Figure 5 (supplementary material). The thermal ellipsoids have been drawn to include 50% of the probability distribution, and, for clarity, the hydrogen atoms have been omitted.

Bond distances and interbond angles, together with their estimated standard deviations, are given in Table VI. The results of weighted least-squares planes calculations are listed in Table VII, and intramolecular contacts less than 3.0 Å are given in Table VIII in the supplementary material.

The Co–N distances, which range from 1.931 (12) to 1.959 (11) Å and average 1.945 Å, are similar to those found for many other Co(III)–amine derivatives, e.g., 1.96 (2) Å in *trans*-$[Co(en)_2Cl_2]S_2O_6 \cdot H_2O$,[31] 1.94 (2) Å in *trans*-$[Co(en)_2(SO_3)(NCS)] \cdot 2H_2O$.[32] Likewise the N–Co–N angles [N(1)–Co–N(2), 85.2 (5)°; N(3)–Co–N(4), 85.3 (5)°] are less than 90° and are typical of Co(III)–ethylenediamine rings. The distance C(3)–C(4) [1.385 (27) Å] is abnormally short. Although it was not possible to resolve C(4) into more than one peak, it seems most probable that C(4) is disordered [as shown by the high thermal motion perpendicular to the N(1)–Co–N(2) plane], and that the distance C(3)–C(4) represents the time averaged distance between two possible ethylenediamine ring conformations. The ethylenediamine ring containing N(3) and N(4) has the usual skew conformation, with C(5) and C(6) being on opposite sides of the plane defined by N(3), Co, and N(4).

The distance Co–O(1) [1.905 (8) Å] is in excellent agreement with previous observations for carboxyl groups coordinated to cobalt(III), e.g., 1.914 (6) Å for the Co–O(gly) distance in the Δ-β_1-(*R*,*S*)-$[Co(trien)(gly)]^{2+}$ ion.[33] As expected, the distance Co–O(2) is significantly longer [1.934 (8) Å], and this lengthening of 0.03 Å presumably reflects the differing σ bond radius of the oxygen atom in sp^2 and sp^3 hybridization states.

The C–O bonds within the coordinated carboxyl group of the methylmalato ligand [C(1)–O(1), 1.256 (14) Å; C(1)–O(11), 1.243 (14) Å] are equal within experimental error. It is more usual for the carboxyl group to be polarized, with the larger C–O bond being to the coordinated oxygen atom, e.g., in (4,5-dihydroxy-4,5-dimethyl-1-pyrroline-2-carboxylato)cobalt(III) ion[34] the distances are C–O(coordinated), 1.276 (9) Å, and C–O(free), 1.228 (7) Å. The remaining bond lengths within the methyl malate ion are all within experimental error of their expected values as follows: C(2)–O(2) [1.458 (15) Å]; C(24)–O(23) [1.457 (20) Å], expected value 1.426 (5) Å;[35a] C(1)–C(2) [1.552 (19) Å], C(21)–C(22) [1.500 (21) Å], expected value 1.506 (5) Å;[35b] C(22)–O(22) [1.198 (16) Å], expected value 1.233 (5) Å;[35c] C(22)–O(23) [1.359 (18) Å], expected value 1.358 (5) Å.[35c]

Kinetics. The cyclization of the *cis*-$[Co(en)_2(methylmaleato)]^{2+}$ ion was followed spectrophotometrically at 356 nm under a variety of buffer and pH-stat conditions between pH 6.5 and 12 at 25 °C. Plots of $\log(A_\infty - A)$ against time were linear for at least $3t_{1/2}$. In pH–stat conditions, the pH rate constant profile is sigmoidal as shown in Figure 6 and Table IX in the supplementary material. In the presence of buffers, the same sigmoidal pattern was observed but the rates were greater than for the pH-stat conditions. They increased further as the buffer concentration increased except in the high base region where the pH-stat and buffer data merged. It can be seen clearly from the data (Figure 6) that the best buffer catalysts are the weakest bases and the cyclization is a general acid-catalyzed process. The cyclization was also followed by ^{1}H NMR spectroscopy albeit where the complex concentration was greater and the rate measurements agreed within a factor of 2 with those measured spectrophotometrically at the same pH. The pH-stat data (pH < 11) gives an observed rate law of the form

$$k_{obsd} = \frac{a}{b + c[H^+]}$$

A similar pattern of reactivity was observed for the cyclization of the *cis*-$[Co(en)_2(OH)(ethylfumarato)]^{2+}$ ion. The results of

(31) Foss, O.; Moroy, K. *Acta Chem. Scand.* **1965**, *19*, 2219–2228.
(32) Baggio, S.; Becker, L. N. *J. Chem. Soc., Chem. Commun.* **1967**, 506–508.
(33) Buckingham, D. A.; Creswell, P. J.; Dellaca, R. J.; Dwyer, M.; Gainsford, G. J.; Marzilli, L. G.; Maxwell, I. E.; Robinson, W. T.; Sargeson, A. M.; Turnbull, K. R. *J. Am. Chem. Soc.* **1974**, *96*, 1713–1725.
(34) Robertson, G. B.; Whimp, P. O. *Aust. J. Chem.* **1975**, *28*, 2129–2135.
(35) *Chem. Soc. Spec. Publ.* **1965**, *No. 18*, (a) 5205, (b) 5155, (c) 5215.

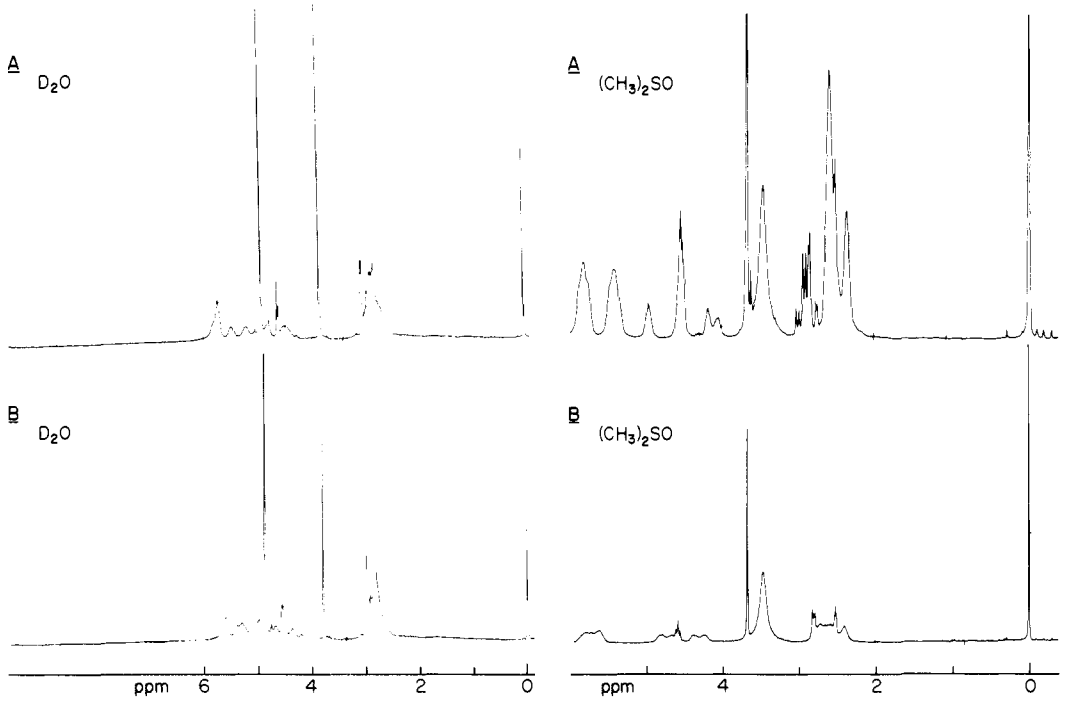

Figure 9. ^1H NMR spectra (200 MHz) of the diastereoisomer of *cis*-$[Co(en)_2(methylmalato)]^+$: (A) less soluble, (B) more soluble.

the kinetic study for this ion are given in Figure 7. They show that the primary difference between the two isomers is ca. a 10^3 lower rate of cyclization for the fumarato complex under comparable conditions.

Analogous Substrate Reactivity. A crude comparative study of the reactions of sodium methyl maleate, sodium 2-chloropropenate, sodium *trans*-3-chloropropenate, sodium ethyl fumarate, and sodium propenate with *trans*-$[Co(1,3\text{-propanediamine})_2(OH)(OH_2)](ClO_4)_2$ was carried out. This cobalt complex has the merit that water exchange is rapid and the carboxylate ligand is captured readily, leading to intramolecular attack by the coordinated OH^- ion at the alkene center and overall hydration of the alkene. Figure 8 shows the ^1H NMR spectra for solutions of the hydroxoaqua complex with the alkene carboxylates over various intervals. The cyclization of the methyl maleate ion was relatively rapid, $t_{1/2} \sim 1$–2 min. However, the 2- and 3-chloropropenoate ions reacted more slowly, and the propenoate ion appeared totally unreactive. With the last, no cyclization was observed before the mixture decomposed over weeks.

The methyl maleate and 3-chloropropenoate cyclized to produce the typical low-field pattern for the exo-cyclic methylene protons of the five-membered chelate products. The 2-chloropropenoate ion reacted somewhat more slowly (<10-fold) than the 3-isomer, and the failure to see the growth of a methyl signal in the vicinity of 1–2 ppm implied that a five-membered ring cyclization had not occurred. However, the disappearance of the doublet due to the protons of the alkene (6–7 ppm) and the appearance of a multiplet at ~3 ppm were consistent with hydration of the alkene to form a six-membered chelate with an endo-cyclic methylene group.

Product Distribution. Under pH-stat conditions at pH 7.1, cyclization of the *cis*-$[Co(en)_2(OH)(methylmaleato)]^{2+}$ ion produced the two diastereoisomeric (*R*)- and (*S*)-malato complexes as well as *cis*-$[Co(en)_2(OH)(methylfumarato)]^+$ ion, Figure 3. The crystallographic analysis identifies one diastereoisomer as a five-membered malato chelate and we presume from the similarity of the ^1H NMR spectra that both are of this form and not a mixture of five- and six-membered malato chelates. Chromatography using Sephadex SP C25 cation-exchange resin and acetate buffer (0.1 M, pH 4.4) separated the fumarato complex from the diastereosiomeric pair since the former elutes as a 2+ ion whereas the malato complexes elute as 1+ ions. This separation arises because the pK_a for the coordinated hydroxo group of the chelated malato complex is 2.75, whereas that of the aquafumarato complex is ~7. Separation of the latter was not achieved by chromatographic methods, but they were parted by crystallization of their perchlorate or bromide salts. However, the ratio of the two diastereoisomers was readily assessed by ^{13}C or ^1H NMR spectroscopy, and the product ratios for the cyclizations were determined by this route coupled with cobalt atomic absorption spectroscopy.

In the presence of buffers at pH 7.1, the cyclization of the *cis*-$[Co(en)_2(OH_2)(methylmaleato)]^{2+}$ complex produced an increasing ratio of methylmalato/methylfumarato complex with increasing buffer concentration. The results are summarized in Table X. Over the pH range 7.1–10 using pH-stat conditions, the methylmalato/methylfumarato ratio was essentially unaltered. The diastereoisomer ratio Λ-S/Λ-R was determined by using deuterated complexes as discussed later, and these values also appear in Table X.

Tracer Studies. Labeled *cis*-$[Co(en)_2(^{18}OH_2)(methylmaleato)]^{2+}$ ion was recovered by the freeze-drying technique after acid hydrolysis of *cis*-$[Co(en)_2(methylmaleato)]^+$ ion in 0.1 M CF_3SO_3H containing 10 atom % $^{18}OH_2$. Subsequent cyclization at pH 13 gave the chelated malato complex, isolated finally as the bromide. In the mass spectrometer, malic acid was distilled from the Co^{3+} ion before ethylenediamine and the EI mass spectrum displayed prominent peaks at *m/e* 89, 99, 103, and 117. These were attributed to loss of $COOCH_3$, OCH_3 plus OH_2, COOH, and OCH_3, respectively, from the parent ion.[36] An enrichment of 5 (±2) atom % ^{18}O was observed for *m/e* 91, 105, and 119, consistent with the incorporation of at least some ^{18}O label, whereas *m/e* 99/101 showed no such enrichment consistent with loss of $^{18}OH_2$ from the parent. The result clearly shows that at least some of the reaction has occurred by attack of the coordinated OH^- ion, and the loss of expected label could be attributed to exchange of coordinated $^{18}OH_2$ with solvent $^{16}OH_2$ before cyclization could be effected. Certainly, the label in the product cannot be ascribed to residual $^{18}OH_2$ from the labeled solvent in the freeze-dried product; the dilution factor is too large.

The stereochemistry of the addition of a deuteron to the cyclized carbanion was also investigated by carrying out the cyclization in D_2O. ^1H NMR spectra of samples of the less and more soluble diastereoisomers of $[Co(en)_2(methylmalato)^{2+}$ ions were recorded at 200 MHz. The less soluble diastereoisomer exhibited an ABX

(36) MacLeod, J. K., private communication.

Table X. Product Distribution for Intramolecular Cyclization of *ics*-$[Co(en)_2(OH)(methylmaleato)]^+$

$[Im]_t$[a]	% malate	% fumarate	k_{obsd} (s^{-1}) × 10^2
0.2	84	16	4.53
0.1	76	24	3.65
0.05	62	38	2.83
0.025	49	51	2.21
0.01	37	63	1.74
pH-stat	24	76	1.38
pH-stat[b]	27	73	3.44
0.2[c]	2:1		
0.8[c]	2:1		
0.1 M NaOD[d]	9:1		

[a] $[Im]_t$ = total imidazole concentration, pH 7.1, μ = 0.2 M, $NaCF_3SO_3$, 25 °C. [b] pH-stat conditions, pH 8.1. [c] 0.2 M imidazole–$DClO_4$ buffer, D_2O solution, ratio of chelated methylmalato diastereoisomers. [d] 0.1 M NaOD–D_2O solution.

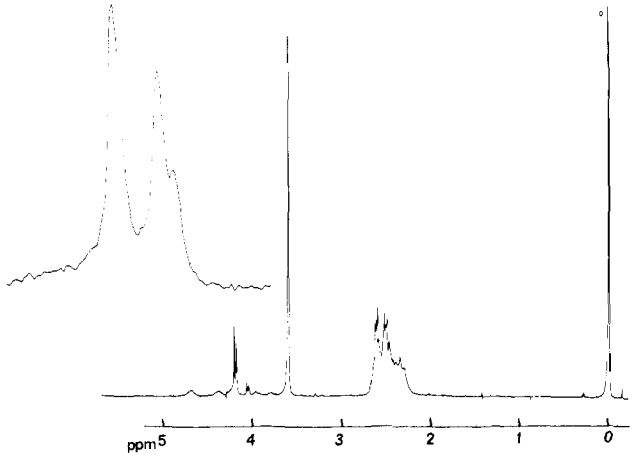

Figure 10. ^1H NMR spectra (200 MHz) of the monodeuterated products from the cyclization of *cis*-$[Co(en)_2(OD)(methylmaleato)]^+$ in 0.1 M NaOD. The insert shows an expanded view of the apparent AB doublet arising from the major diastereoisomer present.

pattern for the methylene and methine protons with J_{AB} = 17.6, J_{AX} = 7.9, and J_{BX} = 3.1 Hz,[37] while the spectrum of the more soluble isomer was essentially a first-order ABX pattern, Figure 9.

Cyclization of *cis*-$[Co(en)_2(OD)(methylmaleato)]^+$ (prepared by acid hydrolysis of the bis(methylmaleato) complex in $DClO_4$–D_2O solution) in 0.2 M imidazole–$DClO_4$ buffer at pH 8 resulted in essentially doublet-pair spectra for the two adjacent protons of the malato d_1 ion in the deuterated diastereoisomers. The 200-MHz ^1H NMR spectrum of the mixture indicated a ratio of 2:1 for the diastereoisomers assessed from the peak heights of the apparent doublet pairs. This ratio was not altered after using deuterated 0.8 M imidazole buffer to effect cyclization at the same pH. However, cyclization of *cis*-$[Co(en)_2(OD)(methylmaleato)]^+$ in 0.1 M NaOD medium led to a 9:1 ratio of deuterated diastereoisomers.

The deuterated less-soluble diastereoisomer was isolated by fractional crystallization. Its ^1H NMR spectrum indicated a simplified ABX doublet for the monodeuterated malato moiety with $J_{AB} \sim 4.4$ Hz, but in higher dispersion (200 MHz), the apparent doublet split into two doublets of unequal intensity (Figure 10) in D_2O. This result implies that protonation is not stereospecific and that both diastereotopic sites were partially deuterated. The same lack of specificity is evident in both the high base and the imidazole buffer experiments. Using Me_2SO-d_6 as solvent for the ^1H NMR spectroscopy, the diastereotopic methylene proton signals became better separated and the lack of specificity in the deuteration step was even more evident.

(37) Banwell, C. N. "Nuclear Magnetic Resonance for Organic Chemists"; Mathieson, D. W., Ed.; Academic Press: London, 1967, p 85.

Scheme I

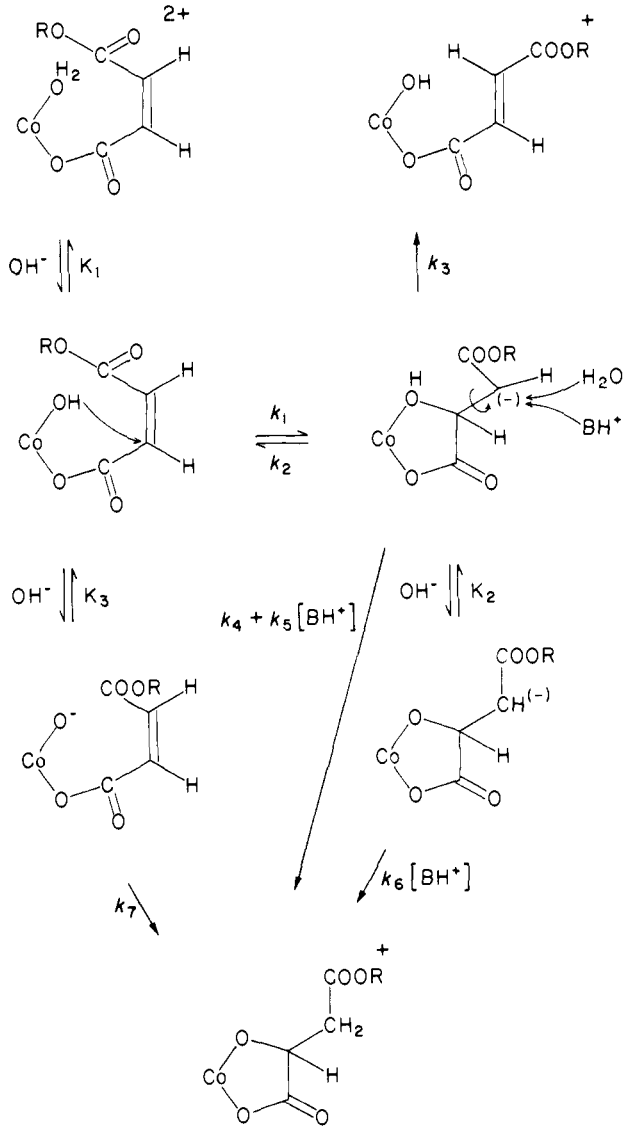

Discussion

In the absence of buffer acids, the results show a rapid intramolecular addition of coordinated OH^- to the coordinated maleate ester to give a five-membered chelate of malic acid ester bound through the hydroxyl and a carboxyl group along with the fumarato isomer of the reactant. The coordinated fumarate ester undergoes the same type of reaction but ~1000-fold more slowly; hence, it can be observed as a product from the reaction of the maleato ester.

The cyclization displays a complicated buffer pH rate profile, Figure 6. Up to pH 7.5, the rate is essentially first order in OH^- for each buffer system. This variation is ascribed to the gradual deprotonation of the coordinated water molecule. In the pH range 8–11, the cyclization appears essentially independent of pH but still shows a marked dependence on the buffer system and the buffer concentration. The reaction is clearly general acid catalyzed, with the strongest acids being the best catalysts. In the presence of the conjugate acid, e.g., imidazolium ion, not only does the rate of cyclization increase but the amount of fumarate produced diminishes and the diminution of this product is linearly related to the concentration of imidazolium ion at constant pH, Table X.

In the high pH region (11–14) the cyclization becomes first order in OH^- again and apparently independent of buffer. It also becomes more stereospecific in the production of malato isomers, and no fumarato product was observed. This change implies a change in the rate-determining step for the cyclization.

These results and the kinetic data are incorporated in the mechanism shown in Scheme I. The scheme requires a rapid intramolecular addition of the coordinated OH^- (k_1) to the alkene C atom β to the carboxy ester function followed by rate-determining protonations of the carbanion generated at the α-carbon atom (at pH < 11). The carbanion generated by the Co–OH addition competitively rotates about the C_α–C_β bond, captures a proton from H_2O or the conjugate acid BH^+ (k_4, k_5, and k_6), and dechelates by C–O cleavage ($k_2 + k_3$) to regenerate coordinated OH^-. The dechelation and rotation yield reactant (k_2) and fumarato product (k_3). Capture of a proton by the carbanion yields the $R + S$ chelated malato ions. The reaction is irreversible at this point since the chelated malato products prefer to lose a proton from the coordinated OH group ($pK_a = 2.74$) which then makes it much more difficult to remove a proton from the carbon adjacent to the carboxy ester group.

The simplest mechanism which accounts for all the data is that shown in Scheme I. Assuming that the steady-state approximation holds, the derived rate law has the form

$$k_{obsd} = \frac{k_1K_1}{[H^+]^2 + K_1[H^+] + K_1K_3}\{([H^+]^2(k_3 + k_4) + k_7K_3[H^+](k_2 + k_3 + k_4) + (k_5[H^+] + K_2k_6)(k_7K_3 + [H^+])[BH^+])/([H^+](k_2 + k_3 + k_4) + (k_5[H^+] + K_2k_6) \times [BH^+])\}$$

In the pH-stat conditions at pH <11, this reduces to

$$k_{obsd} = \frac{k_1K_1(k_3 + k_4)}{K_1(k_2 + k_3 + k_4) + (k_2 + k_3 + k_4)[H^+]}$$

and a plot $1/k_{obsd}$ vs. $[H^+]$ yields a slope of $(k_2 + k_3 + k_4)/(k_1K_1(k_3 + k_4))$ and an intercept of $(k_2 + k_3 + k_4)/(k_1(k_3 + k_4))$. A least-squares fitting procedure gave

$$\frac{k_1K_1(k_3 + k_4)}{(k_2 + k_3 + k_4)} = 1.8\times 10^{-9}$$

and from the intercept, a pK_1 of 7.36 was calculated compared with the measured value of 7.14. This in turn gave a limiting rate constant of 4.0×10^{-2} s^{-1} compared with that observed of 4.4×10^{-2} s^{-1}.

The product distribution in the pH-stat conditions shows that the malate/fumarate ratio ($k_4/k_3 = 0.32$) is independent of pH as required by the rate law. In the presence of buffer, the ratio R = malate/fumarate = $(k_4 + (k_5 + k_6)[BH^+])/k_3$, and a plot of R vs. $[B_t][H^+]/(K_B + [H^+])$ (where B_t = total concentration of the B species and K_B is the pK_a of $[BH^+]$) is linear over the range of BH^+ used. This analysis produces $(k_5 + k_6)/k_3 = 44$ and $k_3/k_4 = 3$ consistent with the acid-independent ratio.

For the conditions at pH <11 in the presence of buffers, the observed rate law has the form

$$k_{obsd} = \frac{a + b[BH^+]}{c + [BH^+]}$$

at constant $[H^+]$, and this can now be interpreted as

$$a = \frac{k_1K_1}{K_1 + [H^+]}\cdot\frac{[H^+](k_3 + k_4)}{k_5[H^+] + K_2k_6}$$

$$b = \frac{k_1K_1}{K_1 + [H^+]}$$

$$c = \frac{[H^+](k_2 + k_3 + k_4)}{k_5[H^+] + K_2k_6}$$

The data in Table IX and Figure 6 have been used to iteratively solve this equation for the parameters at each $[H^+]$. The fit of k_{calcd} to k_{obsd} is shown in Figure 11. A full derivation of the rate law and kinetic analysis is included in the supplementary material.

The rate constants and rate constant ratios that we can extract from this scheme with the data available are given in Table XI. The first-order rate constant k_1 for the addition of coordinated OH^- to the alkene is quite large at 0.21 s^{-1} and the observed rate

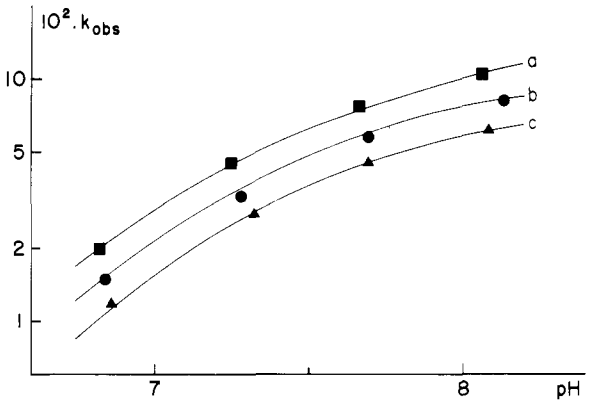

Figure 11. Dependence of k_{obsd} on $[B_t]$ (the total buffer concentration) for imidazole buffers in the range pH 6.5–9. The solid lines were calculated from the equation $k_{obsd} = (a + b[B_t]/(c + [B_t])$ at each $[H^+]$. The experimental points are given for (a) 0.2 M (■), (b) 0.1 M (●), and (c) 0.05 M (▲) imidazole. See supplementary material for full details.

Table XI. Rate Constants and Rate Constant Ratios for Reaction Scheme I

$k_1 = 0.2$ s^{-1}	$(k_5 + k_6)/k_3 = 44$
$k_2/k_3 = 6$	$(k_5 + k_6)/k_2 = 7$
$k_2/k_4 = 18$	$(k_5 + k_6)/k_4 = 120$
$k_3/k_4 = 3$	$k_2/K_2k_6 \sim 3 \times 10^6$
pK_1 calcd = 7.3	$k_7 \sim 10^6$–10^7 s^{-1}
pK_1 obsd = 7.14	assuming $K_3 \sim 10^{-19}$–10^{-20}

at high imidazolium ion concentration approaches this limiting condition. Another factor which emerges is that ring opening to maleate (k_2) is ca. 6-fold faster than the fumarate formation (k_3) and is faster still than malate production via the protonation by H_2O (k_4). In short, the intramolecular cyclization and dechelation are rapid. Compared with hydration of the uncoordinated half-ester under the same pH conditions, it is at least 10^7-fold faster, despite the fact that the coordinated OH^- is a $\sim 10^7$-fold weaker base bound to the metal ion. Of course, it is also true that in the pH 7–8 region, the concentration of OH^- is small relative to CoOH. However, even discounting this aspect, the reaction is remarkably efficient. It is also remarkably regiospecific, and only the five-membered chelate is formed with both fumarate and maleate esters. An explanation for this regiospecificity is offered below.

Unfortunately, we cannot extract K_2, the equilibrium constant for deprotontion of the OH group in the carbanion chelate. It would be expected to be smaller than K_a for the chelated malate product ($pK_a = 2.75 \pm 0.03$ at 25 °C, μ = 1 M, $NaNO_3$), but it is not clear by what amount. It would not seem unreasonable, however, that the pK_a of OH on the carbanion **4** could be as low as 8–9, making such a route accessible. Certainly it appears to be a necessary path in order to fit the kinetic and product distribution results.

The path in the high base region is characterized by the lack of dependence on the buffers, a change in the stereospecificity for the formation of the malato products, and its first-order dependence on $[OH^-]$. Two possibilities arise immediately. One is prior deprotonation of the coordinated OH^- followed by attack of the coordinated oxide ion as the rate-determining step. The basicity of the resulting carbanion **5** would be expected to be greater than for the O-protonated species **4**, and protonation of the C center could then be expected to be faster than the rate-determining addition of the oxide ion. The only problem in this path is the pK_a of the coordinated OH^-.

Assuming that the pK_a value of $OH^- \rightleftarrows O^- + H^+$ is 25,[38] a reasonable estimate for the pK_a of the coordinated OH^- would be 19–20 given the differences shown in Table XII. Also between pH 12 and 14, the reactivity of CoO would need to be $\sim 10^6$-fold

(38) Bell, R. P., "The Proton in Chemistry", 2nd ed.; Chapman and Hall: London, 1973; p 92.

Table XII

	pK_a
$OH \rightleftharpoons O^{2-} + H^+$	25[a]
$H_2O \rightleftharpoons OH^- + H^+$	15.8[a]
$H_3O^+ \rightleftharpoons H_2O + H^+$	-1.7[a]
$cis[Co(en)_2(OH)_2maleato]^{2+} \rightleftharpoons cis[Co(en)_2(OH)maleato]^+ + H^+$	7.14[b]
$cis[Co(en)_2(OH)maleato]^+ \rightleftharpoons cis[Co(en)_2(O)maleato] + H^+$	~19-20

[a] Thermodynamic values.[38] [b] This work.

greater than CoOH which is consistent with the anticipated pK_a difference. It follows that the coordinated oxide ion could be a feasible route.

The second possibility is OH^--catalyzed proton transfer from coordinated OH^- to the carbanion immediately following the addition. The limiting step for this reaction would seem to be addition of the HOCo in the first instance (0.21 s^{-1}), and since the base-catalyzed path does exceed this rate constant such a proposal can be eliminated. Although hydroxide ion could remove a proton from CoOH synchronously with the addition, the improbability of the coincidence of the events militates against such a path.

Finally, it is likely that the carbanion is stabilized by delocalization over the methyl carboxy group. This would account

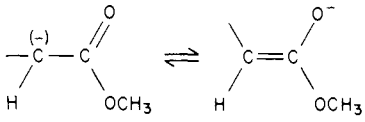

for the relatively slow protonation rate, and it would also assist the addition of the nucleophile. Some of the pattern of events parallels that observed for the cyclization and isomerization of $[(H_2O)_5Cr$ maleate $H]^{2+}$. A five membered chelate malato complex was proposed, and both products increased as the acid concentration decreased. The mechanism argued for the Cr(III) chemistry involved rate-determining H^+ transfer from a coordinated water to the olefin center which generated a carbonium ion very susceptible to attack by the coordinated nucleophile, CrOH. The current chemistry would imply the inverse mechanism, rate-determining attack of CrOH followed by rapid protonation. Both paths are consistent with the acid dependence, but it is not likely that the protonated buffer base or water would effectively protonate the olefin in the cobalt complexes.

Electronic Effects. Superficially, there is an expectation that analogous alkene systems such as coordinated acrylate ion could be hydrated by this route. The charge on the carboxylate ion is largely neutralized once coordinated and a nucleophilic addition could take place at the β-carbon atom. Experimentally, however, hydration was not observed although hydration of analogous 2-chloro- and 3-chloroacrylate complexes did occur; the former yielding a six-membered chelate, the latter a five-membered chelate albeit more slowly than the maleato ester cyclization, Figure 12. Clearly, the cyclization is governed by the substituents exo to the ring formed and the coordinated carboxylate ion has little if any influence on the reaction.

The origin of the regiospecificity appears to reside in the stereochemistry of the activated complex to form the chelate, Figure 13, and the interaction of the electronic systems involved. The alkene π system has to be oriented approximately orthogonal to that of the bound carboxyl ion. In this orientation, the bound carboxyl does not activate the alkene to the nucleophile. However, a carboxy ester group exo to the ring has no problem orienting itself to be coplanar with the alkene moiety. It thereby creates maximum overlap between the two π systems, and addition takes place at the β-C atom, i.e., the C adjacent to the bound carboxyl to give the five-membered chelate.

Similar activation effects were observed for both chloroacrylate systems even though the degree of activation was less than for the maleate half-ester. In general, the degree of activation parallels that observed in the normal organic chemistry where the ester group is superior to the chloro group and the β-carbon accepts

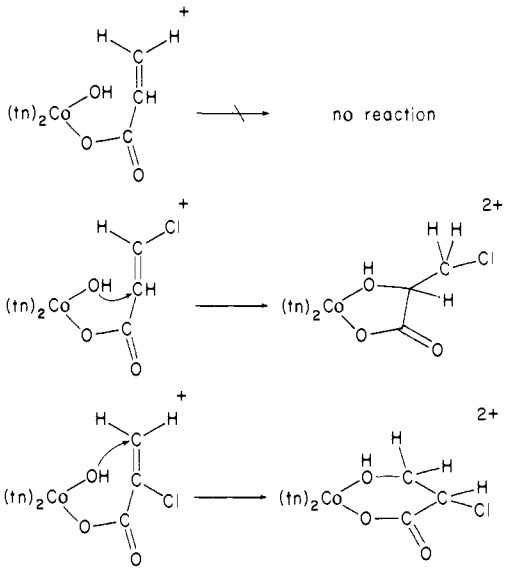

Figure 12. Intramolecular cyclizations of *cis*-$[(tn)_2Co(OH)(alkene)]$ complexes to produce five- and six-membered ring chelates.

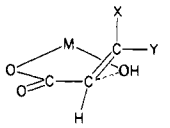

Figure 13. Stereochemistry of the addition of bound OH^- to the alkene.

the nucleophile. It is only the stereochemistry of the activated complex which modifies the expected organic chemistry, and similar constraints must be pertinent in modifying other intramolecular reactions conducted about the metal ions.

Stereospecificity. The two diastereoisomeric methyl malate chelates arise from the two different orientations of the alkene plane relative to the coordinated OH^- attached to the chiral Co center, i.e., *pro-R* or *pro-S*. Since the kinetic analysis implies a pseudoequilibrium situation up to pH 10, it would not be unreasonable if the distribution $(\Lambda\text{-}(S)/\Lambda\text{-}(R) \sim 2)$ reflected essentially the isomer equilibrium distribution for this system. This notion is consistent with at least an analogous chelated amino acid system at equilibrium[39] $\Lambda[Co(en)_2\text{-}(S)valinato]^{2+}/\Lambda[Co(en)_2\text{-}(R)valinato]^{2+} = 1.7 \pm 0.14$ at 34.3 °C. Here, the equilibrium position was attributed to the degree of interaction between the substituent on the chiral C center and the orientation of the two chelate rings about the Co^{3+} ion.

In the high pH path, however, the stereospecificity of the addition is substantially greater, $\Lambda\text{-}(S)/\Lambda\text{-}(R) \sim 9$, which clearly does not reflect a near-equilibrium condition. The planar alkene would interact with more steric compression at the chelates about cobalt for the $\Lambda\text{-}(S)$ form if the addition of the nucleophile was rate-determining. The origin of the effect is the same as for the near-equilibrium situation but more pronounced. Some indication of the differences can be gauged by using Dreiding molecular models and earlier discussion on this issue.[40]

Under these circumstances, protonation must be much more rapid and correspondingly the species to be protonated much more basic than that for the pH 8–11 pathway. This could be readily accounted for by the basicity of the carbanion with $Co^{3+}\text{–}O^-$ added compared with that derived by adding $Co^{3+}\text{–}OH^-$.

The other aspect of stereospecificity is the stereochemistry of H^+ addition. For both the pH-independent and high base paths, some specificity (60:40) for one diastereotopic form was observed. However, no definite conclusion has been reached on how the preference arises. The coupling constant ($J \sim 4.4$ Hz) was consistent with rotamers generated by both cis and trans addition

(39) Buckingham, D. A.; Marzilli, L. G.; Sargeson, A. M. *J. Am. Chem. Soc.* **1967**, *89*, 5133–5138.

(40) Hammershøi, A.; Sargeson, A. M.; Steffen, W. L. *J. Am. Chem. Soc.* **1984**, *106*, 2819–2837.

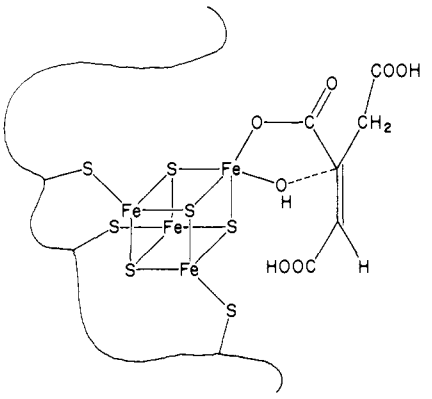

Figure 14. Feasible binding of substrate and nucleophile in the active $[Fe_4S_4]^{2+}$ cluster of aconitase.

of H^+ at the alkene face relative to the addition of the nucleophile. It could also be accommodated by rotation about the C_α–C_β bond after addition of the nucleophile followed by protonation trans to the nucleophile. Delocalization of the carbanion over the methylcarboxy group could also lead to addition of the proton either *R* or *S* without rotation about the C_α–C_β bond. Both routes appear acceptable for the pH-independent path, but only the former route seems viable for the high pH path where nucleophile addition appears to be rate-determining and negligible ring opening occurs.

Relevance to Aconitase Chemistry. It has been inferred in the introduction that the enzyme chemistry is essentially acid–base and not redox chemistry and that the role of the metal ion is to bind the substrate through an OH group and possibly a carboxyl group. Mössbauer, EPR, and NMR studies all appear to indicate binding of *trans*-aconitate, citrate, and isocitrate to a metal ion.[4-8] Water also appears to be bound to the unique Fe ion in the cluster.[4] It is this iron atom with ferrous character which is readily lost from the cluster to give an $[Fe_3S_4]$ cluster. Reapplication of Fe^{2+} and a reducing agent to the inactive form reactivates the enzyme. Given the detailed and elegant analysis of the data,[4-7] a cluster of the type shown in Figure 14 seems feasible. Such five-coordinate Fe centers in Fe_4S_4 clusters have been observed in structural studies.[41] There is also evidence of rapid substrate binding and OH_2 addition at the unique Fe center and at least five coordination at this site.[3-7] The ferrous character of the center is consistent with such rapid substitution[42] and necessary for turnover of the substrate. These proposals would all be consistent with the implications of the chemistry observed in the models. A displaced thiolate ion might then become the base for removal of the proton from citrate or isocitrate. However, there are numerous other structural possibilities including a six-coordinate Fe site with the thiolate still bound.

The speed of the intramolecular cyclization, its regiospecificity and electronic control, the buffer dependence of the rates, and the rapid dechelation of the carbanion in the model system lead to a simple mechanistic proposal for the enzyme, Scheme II. This proposal merely requires partially protonated *cis*-aconitate to be bound as a monodentate in two ways in rapid equilibrium, one to a terminal carboxylate ion and the other to the central carboxylate ion. A coordinated *cis*-hydroxo group can then attack the activated double bond in each instance, followed by protonation from the enzyme acid group to give citrate in the one instance and isocitrate in the other. In both situations, five-membered cyclizations are prescribed by the model chemistry.

The proposal allows the removal of a proton from citric acid at C(2) on one face of the incipient alkene by an enzyme base and its replacement at C(3) on the opposing face, stereospecifically (2*R*,3*S*). In the two processes, different carboxylates are coordinated at Fe during the addition of the coordinated nucleophile, but the *cis*-aconitate ion could be anchored at the site by the third carboxylate group if it were H bonded to an appropriate site on the enzyme. Such an arrangement would allow it to pivot about the H-bonded terminus in order to add the nucelophile at either face.

Scheme II

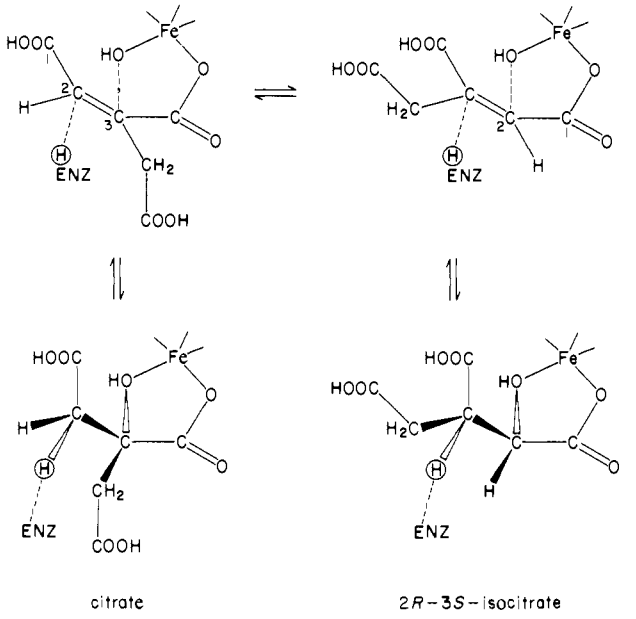

An attractive feature of the proposal is the orientation of the skeleton of C atoms for both modes of coordination. The proximate base which removes the initial proton can also return it to another C atom in the same position. No enzymic conformational change is required to relocate the position of the protonating acid. Only a rapid exchange of coordinated carboxylate ion is involved. Usually, such substitution reactions are fast at high spin Fe^{2+} ($\sim 10^6$ s^{-1}),[41] much faster than the turnover of the enzyme (~ 10 s^{-1}).[8] The models indicate that at least bound OH^- is required as the nucleophile. Coordinated H_2O appears to be inadequate to effect hydration. The pK_a of H_2O bound to a ferrous like iron atom in the cluster could also be around biological pH.[43]

One especially interesting facet of the model cyclization in the pH-stat conditions is that the carbanion dechelates faster than it is protonated. This aspect clearly provides support for a rapid release of coordinated OH^- from the carbanion derived from citric acid to yield the alkene, a process required in the enzyme chemistry. Unfortunately, after the carbanion is protonated in the model system, the reaction is irreversible. Added base then removes a proton from the coordinated OH of the malic acid moiety (pK_a $\sim$ 2.75) rather than from the pendant methylenecarboxy moiety. The deprotonation of the malatehydroxy group thereby makes it much more difficult to deprotonate the methylene group. In this respect, a strategically oriented base in the enzyme could selectively deprotonate the *pro-R*-methylenecarboxy group of citric acid without deprotonating the coordinated alcohol group. In this way, the enzyme can establish reversibility whereas the model chemistry cannot.

Similar selective deprotonation problems apply to the pendant *pro-R*-carboxyl group of citric acid. This group needs to be protonated or H-bonded to the enzyme in order to remove a proton from the adjacent methylene group readily. Also, the aconitate carboxyl bound to the alkene center needs to be protonated or H-bonded to the enzyme in order for the alkene to be activated toward nucleophiles. This effect is observed in the model chemistry or the parent alkene chemistry where it is difficult, if not impossible, to add a nucleophile unless such carboxyls are protonated or esterified. It is for this reason that the half-esters of maleic

(41) Johnson, R. E.; Papefthymiou, G. C.; Frankel, R. B.; Holm, R. H. *J. Am. Chem. Soc.* **1983**, *105*, 7280–7287. Kanatzidis, M. G.; Ryan, M.; Coucouvanis, D.; Simopoulos, A.; Kostikas, A. *Inorg. Chem.* **1983**, *22*, 179–181.

(42) Swift, T. J.; Connick, R. E. *J. Chem. Phys.* **1962**, *37*, 307–320.

(43) The pK_a of $Fe(H_2O)_6^{2+}$ for example is 8.3: Leussing, D. L.; Kolthoff, I. M. *J. Am. Chem. Soc.* **1953**, *75*, 2476–2479.

and fumaric acids have been used in the current studies.

The question of why the enzyme chooses to use a cluster instead of a simple metal ion coordinated to the protein needs to be addressed. A tempting explanation for the need of the cluster lies in its redox characteristic and the possibility of controlling the enzyme through the oxidation states of the cluster and their properties. The Beinert et al. studies show that oxidation of the $[Fe_4S_4]^{2+}$ cluster in the presence of substrate leads to a $[Fe_3S_4]$ cluster and inactivation of the enzyme. However, this cluster can be reduced again with reincorporation of the Fe^{2+} ion and reactivation of the enzyme. In this way, the enzyme might be turned on and off. The use of the redox property to induce a conformational change in the enzyme and thereby trigger the hydration has also been proposed.[44]

Finally, regardless of whether the chemistry described mimics the biology or not in the final analysis, it is clearly an effective way to hydrate alkene centers of this type, and the $[(tn)_2Co(OH)(OH_2)]^{2+}$ ion used could be an effective reagent for this purpose. There are indications that the metal ion exerts substantial constraints on the organic chemistry other than those effects attributed to propinquity and a substitute for a proton. Such effects are probably more common than we have realized and act in both inhibitory and enhancement roles. They clearly need further investigation.

Acknowledgment. We are grateful to Dr. Karl Hagen for stimulating discussions and for the suggestion concerning the use of a displaced thiol, to the Microanalytical Unit of the Australian National University, and the NMR Service at the Research School of Chemistry, Australian National University.

Note Added in Proof. Sir John Cornforth has suggested an alternative explanation for the rate-determining protonation in the cyclization of the maleato and fumarato esters—namely, that general acid catalyzed rearrangement of the enol to the ester would be an equally good if not better description of the process rather than protonation of a "carbanion". The delocalization of the carbanion is alluded to in the discussion but the consequences are not spelled out. A common intermediate for the maleato and fumarato cyclizations could arise and the difference in the rate of cyclization would then come largely from the equilibrium constant for the formation of the enol intermediate from the two isomers.

(44) Ramsay, R. R.; Dreyer, J.-L.; Schloss, J. V.; Jackson, R. H.; Coles, C. J.; Beinert, H.; Cleland, W. W.; Singer, T. P. *Biochemistry* **1981**, *20*, 7476-7482.

Registry No. *cis*-$[Co(en)_2(methylmaleato)_2]ClO_4$, 97430-94-9; *cis*-$[Co(en)_2(ethylfumarato)(Me_2SO)](ClO_4)_2$, 97430-96-1; *trans*-$[Co(en)_2(ethylfumarato)_2]ClO_4$, 97430-98-3; *trans*-$[Co(tn)_2(ethylfumarato)_2]ClO_4$, 97431-00-0; *cis*-$[Co(en)_2(tert\text{-}butylmaleato)_2]ClO_4$, 97431-02-2; $[Co(en)_2(methylmalato)](ClO_4)_2$, 97431-04-4; $[Co(en)_2(methylmalato)]Br_2$, 97431-05-5; $[Co(en)_2(methylmalato)]Br_2 \cdot 2H_2O$, 97431-06-6; *cis*-$[Co(tn)_2(OH)(OH_2)](ClO_4)_2$, 14099-49-1; *cis*-$[Co(en)_2(Me_2SO)_2](ClO_4)_3$, 14781-36-3; *cis*-$[Co(en)_2(OH)(OH_2)](ClO_4)_2$, 14099-49-1; *trans*-$[Co(tn)_2(OH)(OH_2)](ClO_4)_2$, 61634-20-6; sodium methyl maleate, 27750-22-7; sodium *tert*-butyl maleate, 97431-07-7; sodium ethyl fumarate, 55141-86-1; maleic anhydride, 108-31-6; ethylfumaric acid, 2459-05-4; sodium 3-chloropropenoate, 16987-03-4; sodium 2-chloropropenoate, 16987-02-3; sodium propenoate, 137-40-6; aconitase, 9024-25-3.

Supplementary Material Available: Listing of crystal data, Table I, data collection details, Table II, starting phases generated by MULTAN, Table III, details of the course of refinement, Table IV, least-squares planes, Table VII, intermolecular contacts, Table VIII, perspective view of the unit cell, Figure 5, the derivation of the rate law for the intramolecular cyclization of *cis*-$[Co(en)_2(OH_2)(methylmaleato)]^{2+}$, details of the treatment of the kinetic data, and rate constants for the intramolecular hydration of the $[(en)_2Co(OH_2)(methylmaleato)]^{2+}$ ion, Table IX, thermal parameters, Table XIII, calculated hydrogen atom coordinates, Table XIV, and a listing of structure factor amplitudes, Table XV (28 pages). Ordering information is given on any current masthead page.

X-ray Studies on Metal Ion Interactions with Vitamins. 1. Crystal and Molecular Structure of the Tetrakis(μ-acetato)bis(thiamin monophosphate)dirhodium(II) Sesquihydrate Complex: Thiamin Base–Metal Bonding

Katsuyuki Aoki* and Hiroshi Yamazaki

Contribution from the Institute of Physical and Chemical Research, Wako-shi, Saitama 351-01, Japan. *Received April 2, 1985*

Abstract: The crystal and molecular structure of $[Rh_2(acetato)_4(thiamin\ monophosphate)_2] \cdot 1.5H_2O$ has been determined by X-ray diffraction methods. The thiamin monophosphate ligand, a phosphate ester of vitamin B_1, coordinates to the two axial positions of the dirhodium–tetraacetate cage through the pyrimidine ring nitrogen N(1′). Electronic rather than steric considerations, i.e., a high basicity of N(1′), rationalize the metal bonding at this site. The thiamin moiety of the molecule assumes the frequently observed F conformation with $\phi_T = -3°$ and $\phi_P = -81°$. The C(5) ethyl ester phosphate side chain of the molecule is folded back over the thiazolium ring on the same side as the pyrimidine amino N(4′α). The thiamin monophosphate molecule forms a dimeric structure across a crystallographic center of inversion through the three types of interactions between the thiamin moiety and the phosphate group of its pairing molecule; the phosphate anion interacts bifunctionally with the thiazolium ring via a hydrogen bonding with the acidic C(2)H and an electrostatic interaction with the positively charged S(1) atom, and it further contacts, possibly electrostatically, with the pyrimidine ring. Biological implications of this observation and a possible role of the metal ion in the enzymic processes are briefly discussed in connection with the substrate fixation mechanism. The present structure is only the third X-ray example showing the metal bonding to the thiamin base. Crystallographic details for $[Rh_2(C_2H_3O_2)_4(C_{16}H_{23}N_4O_8PS)_2] \cdot 1.5H_2O$: space group $P\bar{1}$, $a = 14.974$ (9) Å, $b = 10.119$ (4) Å, $c = 8.281$ (3) Å, $\alpha = 96.97$ (3)°, $\beta = 74.38$ (4)°, $\gamma = 99.68$ (4)°, $V = 1187$ (1) Å^3, $Z = 1$. The final discrepancy factors R_F and R_{wF} are 0.058 and 0.067, respectively, for 2448 reflections with $F_o > 3\sigma(F_o)$.

Vitamins are well-known as essential nutrients for animal organisms and play a key role in biology.[1] The physiological role of vitamins is now well established, at least for water-soluble ones, as cofactors for a variety of enzymes. These vitamin-dependent

0002-7863/85/1507-6242$01.50/0